UNIVERSITEIT VAN PRETORIA
UNIVERSITY OF PRETORIA
YUNIBESITHI YA PRETORIA

Energy Efficiency in Dual Fluidised Bed Fast Pyrolysis

By Jandri de la Rey

Dissertation submitted in partial fulfilment of the requirements for the degree

Master of Engineering in Chemical Engineering

Department of Chemical Engineering

Faculty of Engineering, the Built Environment and Information Technology

University of Pretoria

Pretoria

South Africa

November 2015

Supervisor: Professor Mike Heydenrych

UNIVERSITEIT VAN PRETORIA
UNIVERSITY OF PRETORIA
YUNIBESITHI YA PRETORIA

CVD 800

Declaration

I, Jan Hendrik de la Rey, hereby declare that this dissertation and every detail of it is my own unassisted work. I submit this dissertation towards the Degree of Master of Engineering to the University of Pretoria. I declare that this work has not been submitted to any other educational institutions for the purpose of examinations, degrees or qualifications.

Candidate signature

Signed at Pretoria on 02 November 2015.

Energy Efficiency in Dual Fluidised Bed Fast Pyrolysis

Abstract

The Combustion Reduction Integrated Pyrolysis System (CRIPS) is a dual fluidised bed fast pyrolyser that was developed at the University of Pretoria for the conversion of biomass waste to biofuels. The dual fluidised bed design allows in situ catalytic upgrading of bio-oil, by providing the conditions required for the regeneration and decoking of catalysts. The first version of the CRIPS process (CRIPS 1) emphasised the need for an energy balance approach to model the pyrolysis process rather than a mass balance. CRIPS 1 experienced severe energy losses and as a result very poor performance was observed. The energy balance was set up in the enthalpy reference level since no shaft work was produced and the entire process was operated under constant atmospheric conditions. The enthalpy balance approach was set up to analyse the process performance and energy efficiencies of a CRIPS process and possibly the bio-oil energy content and yield that could be expected from such a process. The approach was used to derive the bio-oil properties and energy efficiencies for a number of scenarios based on the CRIPS process. The Higher Heating Value (HHV) of the bio-oil was derived using the total energy balance of the CRIPS process. The validity of the approach was confirmed by comparing the derived bio-oil HHV from CRIPS 1 of 14,2 MJ/kg with that of similar processes, in the range of 17-23 MJ/kg, as well as comparison to the operating data and process yields. The enthalpy balance approach was able to accurately model the operation of CRIPS 1 using energy and mass balances and therefore the approach was used in the design of CRIPS 2 to limit heat losses and improve the process efficiency by recovering heat from the exhaust of the combustor. The heat recovery resulted in significant improvements in the efficiency of CRIPS 2 (74%) compared to CRIPS 1 (33%). The final design of the CRIPS 2 process featured an annular design in which the combustion bed is located in a refractory cylinder, with the pyrolysis bed around the refractory. The design allowed for the addition of a heat exchanger inside the combustor which is responsible for the increase in efficiency.

Acknowledgements

The author would like to thank PAMSA and Sappi Southern Africa Ltd for their continued support with facilities, funding and materials, and expresses his gratitude. Gratitude to the Sappi Technology Centre, Pretoria, for the use of their facilities and equipment. Thanks go to MM Projects at the CSIR for the construction of the reactor equipment. Finally, the author would like to thank family and friends for their support during the project, with special thanks to Professor Mike Heydenrych, whose mentorship and guidance was vital to the success of the project.

Contents

Abstract i
Acknowledgements ii
List of Figures iii
List of Tables iii
1 Introduction 1
1.1 Background 1
1.2 Problem Statement and Objectives 2
1.3 Method and Scope 2
2 Literature Review 4
2.1 Biomass 4
2.2 Thermochemical Treatment of Biomass 4
2.3 Pyrolysis 6
2.3.1 Effect of temperature and composition on yields 6
2.3.2 Fast pyrolysis: conditions and requirements 7
2.4 Pyrolysis Process Design 8
2.4.1 Feed pre-treatment and pneumatic delivery 8
2.4.2 Pyrolysis reactor 8
2.4.3 Product recovery section 10
2.5 Heat Recovery 12
2.6 Bio-oil Quality 13
2.7 Upgrading of Bio-oils 15
3 Combustion Reduction Integrated Pyrolysis System (CRIPS) 17
4 CRIPS Process Modelling 24
5 CRIPS 2 Reactor Design 31
5.1 Principles and Design Considerations 31
5.2 Reactor Design 32
5.2.1 Fluidised beds 32
5.2.2 Heat loss estimation 37

5.3 Conclusions and Recommendations 38
6 Internal Heat Recovery Unit 39
7 CRIPS 2 Process Modelling 45
8 CRIPS 2 Performance Evaluation 47
9 CRIPS 2 with Catalytic Pyrolysis 49
10 Conclusion and Recommendations 53
References 55
Appendix A 59
Appendix B 60
Appendix C 61

List of Figures

Figure 1: Products of thermochemical treatment (Shafizadeh and Chin 1977).....4
Figure 2: Thermal upgrading of biomass (Bridgwater 2011).....5
Figure 3: Dual fluidised bed design (Swart 2012).....9
Figure 4: Grade efficiency curves for gas particle separators (Rhodes 2008).....11
Figure 5: Van Krevelen diagram showing various fuel sources with bio-oil data (adapted by Basu (2010), original work by van Kervelen (1950)).....14
Figure 6: Pyrolysis bed temperature control.....17
Figure 7: Dual bed CRIPS process with sand transfer.....18
Figure 8: ABS model of feeder.....19
Figure 9: Feeder fitted on hopper.....19
Figure 10: Hopper agitator design (Swart 2012).....20
Figure 11: Product separation flow diagram.....21
Figure 12: Product separation and cooling system.....22
Figure 13: View of the process.....23
Figure 14: Enthalpy balance approach for CRIPS 1.....30
Figure 15: Bottom refractory.....33
Figure 16: Distributor design (Batcha, et al. 2013).....35
Figure 17: Pyrolysis gas distributor.....36
Figure 18: Internal heat recovery unit.....40
Figure 19: Sectional design of heat exchanger.....42
Figure 20: Heat exchange profile.....42
Figure 21: Final heat exchanger design.....43
Figure 22: Sectional view with exhaust flow.....44
Figure 23: Enthalpy balance approach for CRIPS 2.....48
Figure 24: CRIPS 2 with triple function chemical looping.....50
Figure 25: CRIPS 2 enthalpy balance approach with catalytic pyrolysis.....52
Figure 27: Van Krevelen diagram with catalysed bio-oils (Basu 2010), (Merckel 2014), (Merckel and Heydenrych 2015).....54

List of Tables

Table 1: Mass yield of products under varying thermal treatments (Bridgwater 2011).....6
Table 2: Energy data from the Boateng study.....26
Table 3: Energy balance analysis for CRIPS 1.....27
Table 4: Performance indicators for enthalpy balance approach (refer to Figure 14).....28
Table 5: System set points and operating conditions.....45

1 Introduction

1.1 Background

The use of biomass, especially wood, is a promising replacement for fossil fuels. Pyrolysis can be used to convert biomass into fuels and other valuable chemicals. It is the high-temperature thermal degradation of materials in the absence of oxygen, and has been the aim of a joint research venture between the University of Pretoria's Department of Chemical Engineering, Sappi Southern Africa (Pty) Ltd and the Paper Manufacturing Association of South Africa (PAMSA).

The project began with interest and funding by an industrial company to develop a scalable system which could convert waste forestry material, specifically sawdust, into valuable and usable products. From the sponsors point of view it was critical to extract and recover the biochar for use in agriculture and to produce a high quality oil for heating purposes. To this effect the project focuses on two methods of pyrolysis, namely microwave pyrolysis (Merckel 2014) and fast pyrolysis (Grobler 2014). Microwave pyrolysis has delivered excellent results with the conversion of *Eucalyptus grandis* (EG) delivering high-quality oils but with incomplete biomass conversion.

The fast pyrolysis research focused on the use of a dual fluidised bed reactor to convert the biomass feed into products with higher energy content and greater value. The reactor comprised a combustion fluidised bed (CB), in which heat is generated, and a pyrolysis fluidised bed (PFB), in which the biomass is converted. The process is referred to as the Combustion Reduction Integrated Pyrolysis System (CRIPS). The first system (CRIPS 1) included a cyclone for biochar recovery, followed by a quencher for the rapid cooling of pyrolysis vapours to extract the bio-oil and non-condensable gases (NCG). The NCG were used as the fluidisation medium in the PFB and as fuel for the CB.

CRIPS 1 experienced severe heat and energy losses which crippled the process performance. Careful modelling of the process was required to determine where losses had occurred and the best improvements that could be made. Typically a mass yield approach

is used to determine process efficiency; however, this approach cannot determine the thermal performance and quality of bio-oil obtained from a process.

1.2 Problem Statement and Objectives

The problems found during experimental runs by Grobler (2014) on the CRIPS 1 process included high energy losses from the fluidised beds and process, difficulty recovering the char product and blockages in the pneumatic feeding of the biomass. These factors prevented accurate results from being obtained. The breakthroughs and performance aspects of CRIPS 1 are given in Section 4.

The research objective was to create a model which can accurately determine the efficiency of a pyrolysis system and predict the quality of the bio-oil produced. The model must account for all energy flows in and out of the process as well as the mass balance associated with the system.

The mass balance includes the oil, NCG, char and water of pyrolysis yield and the CO/CO_2 ratio in the NCG gas is of critical importance to determine the effectiveness of a pyrolysis process. The model of the process was then used to design a reactor and other process alterations for CRIPS 2. These modifications are expected to eliminate or reduce the impact of the problems encountered in CRIPS 1.

1.3 Method and Scope

The limitations of CRIPS 1, together with the results of a literature study, were used to design a model of the CRIPS process. The model was compared to the performance of CRIPS 1 and similar processes to determine its validity. Once the model was verified, the reactor design for CRIPS 2 was done, which included improvements in char recovery and correction of the biomass feeding problems.

The CRIPS process produced no shaft work and operated under constant atmospheric pressure, this allowed the use of a simplistic enthalpy balance approach to model the energy flows in the system. Enthalpy was chosen as the reference energy since most of the

thermodynamic data available on pyrolysis is based in the enthalpy reference level. The model used to design the CRIPS 2 process was then used to derive the expected bio-oil heating value and yields as well as the thermal efficiencies of the system.

2 Literature Review

2.1 Biomass

Biomass is a biological material composed of recently living biological organisms. It can consist of a large variety of materials with different properties. The largest source of biomass produced globally is wood, a lignocellulosic biomass. It contains lignin, cellulose and hemicellulose in varying proportions.

The usable wood or roundwood fraction of wood is used in the paper, pulp and carpentry industries. The remaining wood material is typically burnt for energy production (Heinimo and Junginger 2009). The problem with using this waste biomass directly as an energy source is the reduced higher heating values (HHV) of the material compared to that of conventional fossil fuels such as coal or oil. The low HHV value observed is due to the moisture content and chemical composition (Demirbas 2008). The HHV indicates the energy available per unit mass. When moisture is present a fraction of this energy is used to vaporise the water and the energy is then lost.

2.2 Thermochemical Treatment of Biomass

The CV of biomass can be increased by means of thermochemical treatment to deliver better products. The products are shown in Figure 1.

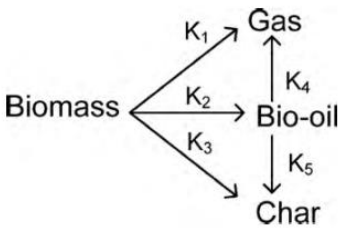

Figure 1: Products of thermochemical treatment (Shafizadeh and Chin 1977).

These products include a char material containing carbon and inorganics, which can be used for heat generation or can be recovered for use as organic fertiliser. The bio-oil is the product of value and can be used as a fuel oil in boilers or gas turbines; however, the value

of bio-oil is its use as a transportation-grade fuel. The oil must, however, be upgraded to make this possible.

The upgrading is typically done by removing the bound oxygen from the oil, which increases the HHV of the oil and produces a non-polar oil allowing distillation or separation. The gases produced are referred to as non-condensable gas or NCG, and can be used for fuel production via Fischer Tropsch or as a direct heat source.

The k symbols illustrate different reaction rate constants which depend partly on the method of thermochemical conversion and the reaction conditions used. Two methods are mainly used for converting biomass into fuels, namely pyrolysis and gasification. These and their products and uses are shown in Figure 2.

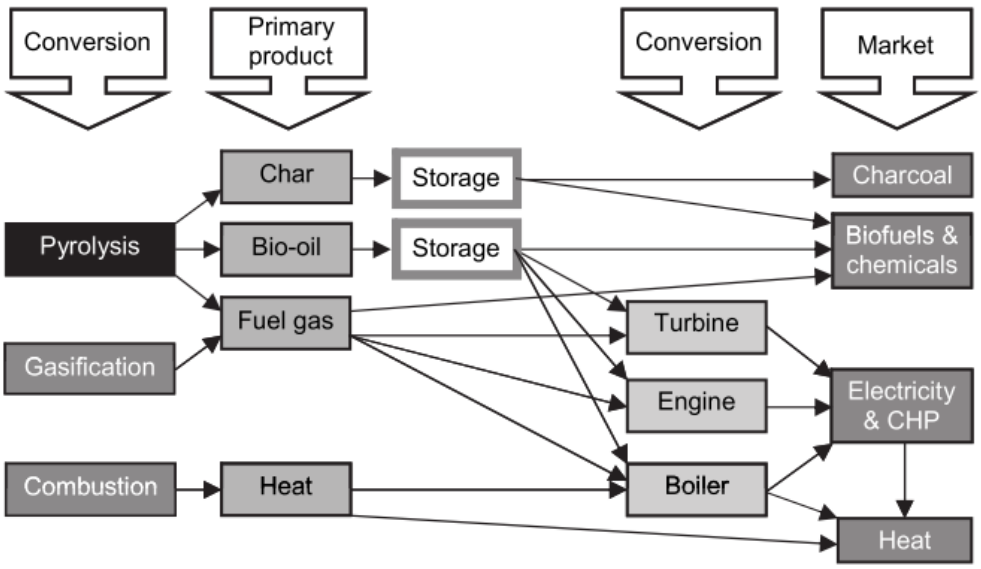

Figure 2: Thermal upgrading of biomass (Bridgwater 2011).

Pyrolysis and gasification can be used as conversion methods by utilising elevated temperatures with specific environments to break down the chemical compounds found in the biomass. The reaction temperature, residence time and temperature of the vapours influence the final product yields. The temperature ranges and product compositions are shown in Table 1.

Table 1: Mass yield of products under varying thermal treatments (Bridgwater 2011).

Mode	Conditions	Liquid	Solid	Gas
Fast	500 °C, short hot vapours, residence time approximately 1 s	75%	12% char	13%
Intermediate	500 °C, hot vapours, residence time approximately 10-30 s	50% in 2 phases	25% char	25%
Carbonisation (slow)	400 °C, long vapour residence time – hours to days	30%	35% char	35%
Gasification	750-900 °C	5%	10% char	85%
Torrefaction (slow)	290 °C, solid residence time approximately 10-60 min	0% unless condensed, then up to 5%	80% solid	20%

As seen in Table 1, the biomass will pyrolise around 500 °C and gasify above 750 °C. The temperature controls the conversion process while the residence time of the vapours controls the liquid yield.

2.3 Pyrolysis

Pyrolysis is the thermal decomposition of a biomass in the absence of oxygen. Careful temperature control is required to yield the best results.

2.3.1 Effect of temperature and composition on yields

As mentioned before, biomass typically contains three main constituent polymers: cellulose, hemicellulose and lignin. Each of these complex polymers reacts differently to the conditions of pyrolysis. During the thermal conversion of these polymers three main reaction mechanisms control the conversion and product yields. These include char formation, depolymerisation and fragmentation (Collard and Blin 2014). These mechanisms are typically followed by secondary reactions, which form smaller-chain hydrocarbons and other functional groups.

It is widely accepted in pyrolysis research that low heating rates favour char formation while high heating rates favour the formation of volatile compounds (Goyal, Seal and Saxena 2008).

2.3.2 Fast pyrolysis: conditions and requirements

The fast pyrolysis of wood requires a 500 °C environment with a vapour residence time of less than 2 seconds to deliver adequate yields of bio-oil and biochar.

The following principles are essential for a high yield of bio-oil (Bridgwater 2011):

- A maximum biomass particle size of 3 mm allows sufficient contact and high thermal energy transfer to the particle.
- The 500 °C reaction temperature favours bio-oil yields.
- The vapour phase residence time should be limited to 2 seconds to prevent secondary reactions illustrated by k_4 and k_5 in Figure 1.
- Rapid removal of biochar. This minimises the cracking of vapours and increases bio-oil yield.
- Rapid cooling or quenching of the vapours to produce the bio-oil product.

The fast reaction time required for bio-oil production presents a problem because the mass transfer, heat transfer and reaction rates all influence the production of bio-oil.

To ensure that the biomass is rapidly heated to the desired temperature, the particle size and moisture content must be closely controlled. The moisture content of the biomass before conversion must be maintained below 10%. This will reduce the heat lost by water evaporation and increase the throughput of the reactor (Bridgwater 2011).

2.4 Pyrolysis Process Design

Fast pyrolysis typically features three systems for the conversion of biomass: the feed pre-treatment, the pyrolysis reactor and the separation or product recovery section.

2.4.1 Feed pre-treatment and pneumatic delivery

The feed pre-treatment is of critical importance to the yield of bio-oil and the efficiency of the pyrolyser. Drying conditions must yield a biomass with a moisture content of 5% to 15% (Jahirul, et al. 2012) which is in agreement with figures suggested by Bridgwater (2011). This reduces the energy lost by water evaporation and also increases the quality of the bio-oil produced.

The conditions for drying which delivered the best product, included a drying temperature of 200 °C for a minimum of 45 minutes followed by the size reduction of the biomass to particles between 2 and 6 mm (Dobele, et al. 2007). This range of particle size ensures a fast reaction time in the reactor and is agreement with the size recommended by Bridgwater (2011). The particle size is also of importance in the pneumatic feeding system if the NCG recycle is used to feed the biomass into the pyrolyser.

The best particle size for pneumatic feeding was found to be 2 mm or less at a superficial gas velocity (SGV) of 25 to 35 m/s. This particle size prevents blockages from forming and the SGV ensures the complete entrainment of the biomass without excessive pressure drops caused by high velocities (Nevill 2001). The method described by Rhodes (2008) on particle fluidisation and entrainment can be used to confirm the accuracy of these findings; however, since the physical properties of the biomass can differ significantly, any result would contain a high degree of error.

2.4.2 Pyrolysis reactor

The typical design of a fluidised bed pyrolyser includes one fluidised bed with electrical elements to provide the energy. The CRIPS process utilises a dual fluidised bed which is essentially two reactor units operating as one. The combustor or CB provides the energy

for pyrolysis and the pyrolyser or PFB in which the biomass is pyrolysed. The PFB maintains an inert environment to prevent combustion. The heat source can be any fuel including the biomass, unrecovered char and NCG products.

The heat is transferred via direct or indirect contact between the two reactors. During direct contact a solid medium such as sand will be heated in the combustor and transferred to the pyrolyser where it comes into contact with the biomass particles. The indirect method allows no flow of material between the units, only the flow of heat. This is, however, more difficult to control and results in lower particle heating rates, which favour char formation (Kersten, et al. 2005). The control of heat transfer via a reactor wall would have to take into account the delay in changing the PFB temperature with a change in the CB temperature. The heating is also only possible from the reactor surface area and therefore as scale up takes place the increased volume of material which must be heated via the surface area available becomes problematic.

If direct heat transfer is used the solid medium must be mobile and therefore both reactors are commonly operated as fluidised bed reactors (Bridgwater and Peacocke 2000). A mechanical linkage can be used to allow the sand to be transferred from the CB (Bed A) to the PFB (Bed B), and it is then returned via a screw conveyor. This limits vapour transfer between beds A and B and prevents oxygen from entering the PFB (Swart 2012). This design is shown in Figure 3.

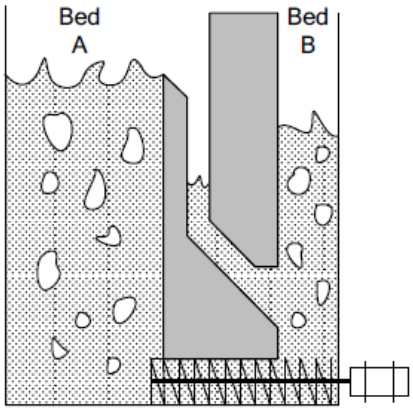

Figure 3: Dual fluidised bed design (Swart 2012)

The design by Swart (2012) supports the validity of biomass pyrolysis as an alternative method to produce fuel, and has resulted in advancements in dual reactor control and bio-oil recovery from hot pyrolysis vapours.

Grobler (2014), continuing the work done by Swart (2012), discovered that the reactor experienced considerable energy losses which reduced the throughput from 20 kg/h to 2 kg/h. The reactor was designed to account for heat losses; however, the actual losses far exceeded the calculated losses from the model. The heat losses limited the research that could be done on CRIPS 1.

The system also proved ineffective at recovering the valuable biochar product – instead it was recycled with the sand into the combustion unit and lost. The remaining char was only partially recovered by the cyclone. This was assumed because large quantities of char were found in the bio-oil recovery section. The results from the work done by Swart (2012) and Grobler (2014) support the feasibility of biomass fast pyrolysis and identified key short comings to be considered in future designs.

In conclusion, the following should be carefully considered in the design of a reactor for fast pyrolysis:

- A PFB temperature of 500 °C with a CB temperature of 900 °C (Grobler 2014)
- A low residence time of vapours at high temperatures, typically less than 2 seconds
- Effective separation between char and sand – char must be entrained in vapours
- A design which allows post-construction alterations to cater for unpredicted heat losses
- The combination of both reactors into one unit: a CB inside an annular PFB

2.4.3 Product recovery section

The product recovery section is an important operation to ensure that quality products are recovered. This section typically includes a cyclone for char and entrained sand recovery

from the hot pyrolysis vapours, followed by a quenching system or heat exchanger which rapidly cools and condenses the vapours into bio-oil and NCG. The NCG and bio-oil can then be separated by hydro-cyclone electrostatic precipitation (ESP) or demisting (Bridgwater and Peacocke 2000).

The fast recovery of char is important to reduce the secondary cracking of vapours. The method of separation must be carefully chosen. The grade efficiencies of different separation methods can be seen in Figure 4.

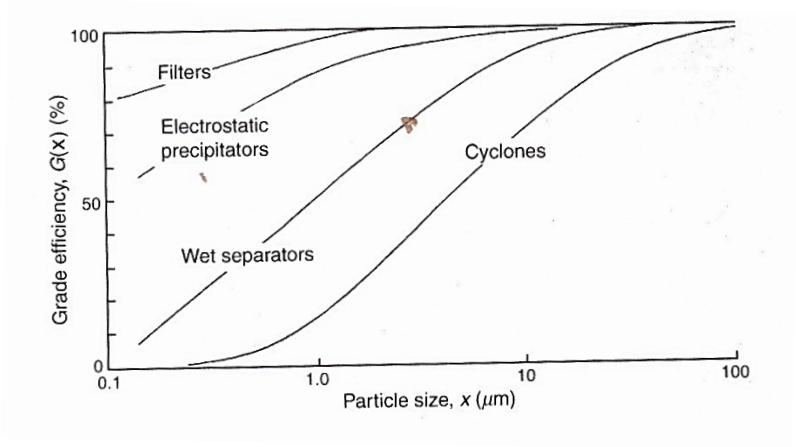

Figure 4: Grade efficiency curves for gas particle separators (Rhodes 2008)

The small particle sizes of char cause cyclones to become ineffective at removing them. As seen in Figure 4, at sizes smaller than 10 μm the efficiency drops below 50%, whereas ESP remains above 50% at sizes as low as 0,1 μm. This, together with the limited data available on the particle size distribution of char which is required for the cyclone design, suggests that ESP is a better option for char recovery (Rhodes 2008).

After the char separation the temperature of the vapours remains a driving force for the cracking reactions, and they must be cooled and condensed rapidly. This was done by quenching in the process designed by Swart (2012). The quenching liquid used was recycled bio-oil mixed with ethylene glycol. The ethylene glycol was used as a starting fluid to fill the cooling system and was used for its high boiling point and it is identifiable as a peak on GC-MS analysis. The hot vapours entered a cylinder via an atomiser which atomised the bio-oil recycle and mixed the vapours and liquid. At this point the liquid acts as a heat sink,

effectively removing all latent and sensible heat from the vapours, condensing all but the NCG (Grobler 2014).

The liquid bio-oil and NCG then enter a hydro-cyclone where they are separated and further stripped of oil by a demister and filter. The NCG is then used as the recycle to the PFB less a purge. The bio-oil is cooled with a water-cooled heat exchanger.

This design returned good results, with the exception of a very high pressure drop on the gas side because of the atomiser. This can be prevented by using a flow atomiser on the liquid side and then spraying it in the same direction as the vapour phase.

2.5 Heat Recovery

The CB was designed to operate at 900 °C to provide acceptable heat transfer and driving force to the PFB and also ensures complete combustion of the fuel. This provides a clean exhaust and also makes it possible to design around a fixed 6% oxygen in the exhaust. This temperature is usually provided by combustion of gaseous or solid fuels. Typically 50% of the heat generated during combustion transfers to the PFB, with another 43% lost in heating the exhaust gas leaving the system at 900 °C. The remaining heat is assumed to be lost.

Grobler (2014) suggested using the energy in the exhaust gas to preheat the combustion air feed and thereby re-using the heat inside the reactor and increasing the heat transfer to the PFB. This ultimately increases the throughput of the reactor. It was also suggested that the flue be used for preheating the gas recycle to the PFB, but the problem with this is that the biomass is pneumatically fed via this gas, so preheating it with 900 °C flue gas would cause an unwanted reaction, and using the flue for drying at that temperature would cause the same problems.

The most feasible option is therefore to use the flue to preheat the air feed in a gas-to-air heat exchanger, followed by the possibility of using the cooled flue gas for drying. Before a design can be done the feasibility of using high-temperature gas must be considered.

2.6 Bio-oil Quality

Fast pyrolysis gives a high yield of oil if the biomass can be heated to temperatures in the range of 400 °C to 550 °C (Bridgwater and Peacocke 2000). This yield of neat bio-oil normally contains large amounts of water and has a high oxygen content in the form of bound oxygenates, which results in a polar neat bio-oil with a low Higher Heating Value (HHV).

The quality of a bio-oil is defined by the water content, oxygen content and HHV of the oil (Heidari, et al. 2013). If bio-oil is meant to be a transportation-grade fuel, the aim is to produce an oil with no oxygen content, similar to crude oil, which has a high HHV (approximately 45 MJ/kg) due to its low oxygen content and saturated hydrocarbons (Basu 2010). The Van Krevelen diagram (adapted by Basu (2010)), shown in Figure 5, is a good method to compare the HHVs and the hydrogen and oxygen content of fuels. The diagram was developed by Dirk Willem van Krevelen as a graphical plot to assess the origin and maturity of petroleum and kerogen (van Krevelen 1950).

The Van Krevelen diagram compares fuels based on their hydrogen-to-carbon ratio (H/C) versus their oxygen-to-carbon ratio (O/C). The quality of the fuel increases as the H/C ratio is increased and the O/C ratio is decreased, illustrated by the red arrow in Figure 5. This increase in quality is accompanied by an increase in the HHV of the fuel as seen with the HHV of petrol of 46,6 MJ/kg compared to that of *Eucalyptus grandis* wood of 18 MJ/kg.

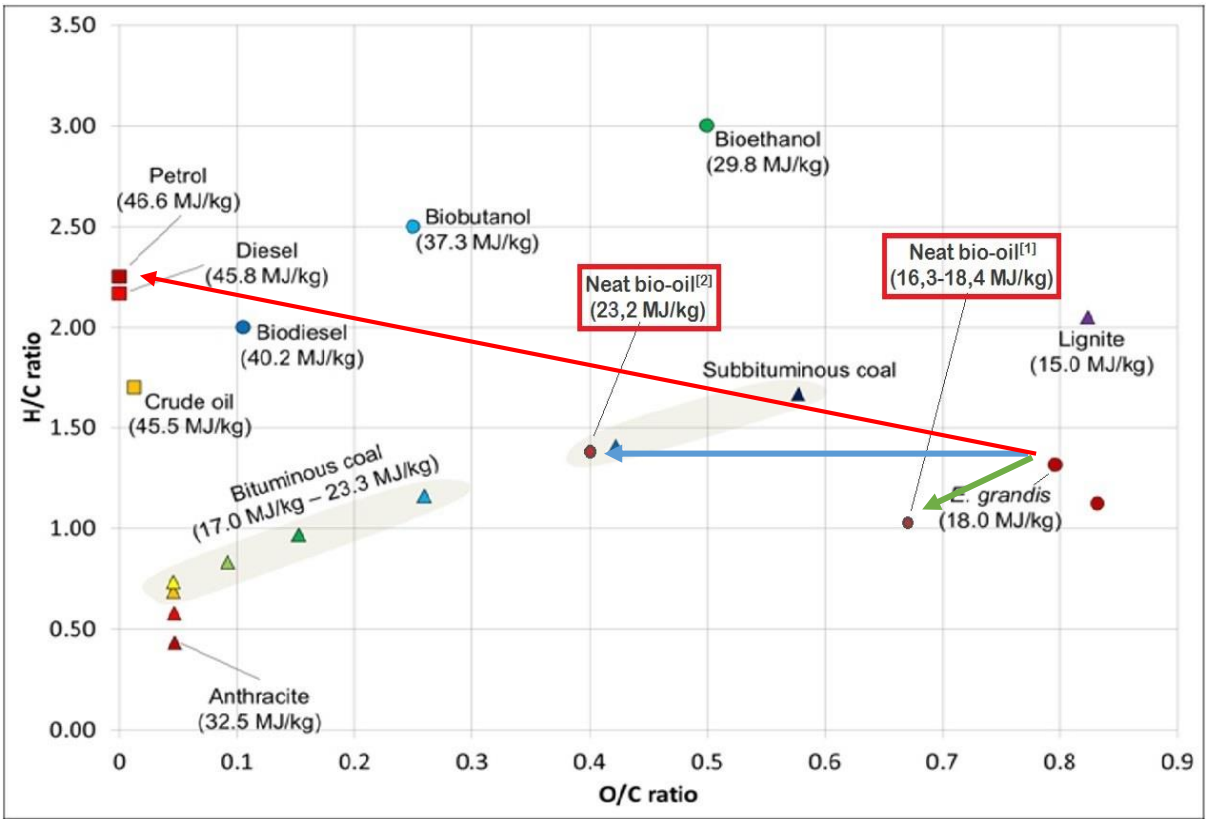

Figure 5: Van Krevelen diagram showing various fuel sources with bio-oil data (adapted by Basu (2010), original work by van Krevelen (1950))

In laboratory processes an inert carrier gas is often used to fluidise the pyrolyser and electric elements are used to supply the heat of pyrolysis (Fernandez-Akarregi, et al. 2013), which is not a feasible approach for commercial operation, since the NCG is diluted in the inert carrier gas and the heating value is lost. The neat bio-oils[1] (Figure 5) typically produced in such processes have HHV's in the range of 16,3-18,4 MJ/kg because of high oxygen to carbon (O/C) ratios (Makibar, et al. 2015).

Neat bio oils[2] (Figure 5) produced by processes that recycle NCG show reduced O/C ratios and increased HHVs compared to bio-oils[1] (Boateng and Mullen 2013). The bio-oil produced by Grobler (2014) was diluted with ethylene glycol as the cooling or quenching medium and as a result the GC-MS analysis and heating value determination was of no value.

2.7 Upgrading of Bio-oils

The need to upgrade bio-oil has prompted research studies and commercial-scale testing of various forms of upgrading in recent years. The aim is to produce a high-quality bio-oil that can be used as a feedstock to conventional petroleum refineries to produce a typical range of fuels, including petrol, diesel, jet fuel and kerosene.

Hydrodeoxygenation (HDO) is the most common upgrading process. It was originally inspired by the hydrodesulphurisation and hydrodenitrogenation processes used in the petroleum refining industry. During HDO upgrading, hydrogen is used to remove oxygen from the oil as water. The method is dependent on hydrogen as an expensive feedstock, which is an economic disadvantage. An alternative is the use of hydrothermal processing, during which hot pressurised water is used to upgrade the oil. The method requires near-critical water to be effective, which is costly to produce (Sharifzadeh, et al. 2015). The processes described above are used in commercial pyrolysis operations such as ENSYN, Dynamotive and KiOR (Butler, et al. 2011), (Meier, et al. 2012). The processes involve the use of costly equipment and materials after the initial pyrolysis operation to upgrade the oils.

An alternative to this is the use of in situ catalysis with the pyrolysis reactor. The catalyst is loaded into the same reactor as the biomass feed. During this process the biomass is pyrolysed and the oil vapours are upgraded in the same reactor unit. The use of bentonite and zeolite in situ catalysis has proved effective in upgrading the oil (Merckel & Heydenrych, 2015); however, due to the nature of the catalyst, the oxygen in the oil is removed as water. This causes a drop in the H/C ratio and also promotes the coking of the catalyst.

The reduction in H/C ratios, seen with zeolite and bentonite, is a step backwards, since the quality of a fuel is decreased with a drop in H/C ratios. A different catalyst is therefore required that can remove oxygen from the fuel as CO_2 (one mole carbon lost from oil for 2 moles of oxygen removed) rather than H_2O (two moles of hydrogen lost for every mole oxygen removed).

The process of chemical looping combustion (CLC) uses a solid oxygen carrier to transfer oxygen between the air and a fuel for combustion, thereby preventing direct contact between the fuel and the air. During the first reaction the metal oxide (MO) supplies the oxygen for fuel oxidation and forms the metal (M). The metal oxide is then regenerated with air in a separate reactor. Fluidised beds are often used for continuous flow processes (Adanez, et al. 2011).

This process can be modified to use MO as a means of upgrading the bio-oil. The use of MOs in LDH-based catalysts (Layered Double Hydroxide) and metal sulphide (MS) are promising alternatives, since the MO captures oxygen in the form of CO_2 to become MCO_3 during a decarboxylation reaction and the MS captures oxygen to form MSO_x, the mechanism is still unclear. As these catalysts become saturated with oxygen they become ineffective and must be regenerated by the burn-off of the captured oxygen. The reducing conditions at high temperatures cause coking of the catalyst, which renders it ineffective within minutes. To solve these problems, a high-temperature oxidative environment with the presence of a carbon source is required to regenerate and decoke the catalyst.

3 Combustion Reduction Integrated Pyrolysis System (CRIPS)

The pyrolysis process, CRIPS, developed at the University of Pretoria, uses a dual fluidised bed fast pyrolysis process, in which heat generated in a combustion fluidised bed (CB) is used to heat a bed of sand. The heated sand then flows over into the pyrolysis fluidised bed (PFB), where it drives the endothermic pyrolysis process. The sand is cooled during this process to the temperature of the pyrolysis reactor and is fed back to the combustor via a screw feeder. This allows the sand to reheat and flow back to the pyrolyser. This process, illustrated in Figure 7, allows accurate control of the PFB temperature, while preventing the transfer of oxygen into the pyrolyser (Swart 2012). The accuracy of the control system can be seen in Figure 6.

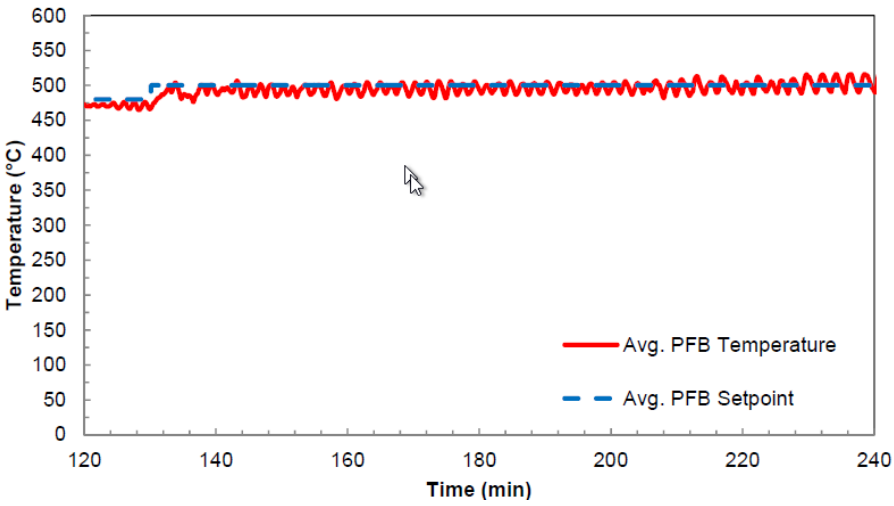

Figure 6: Pyrolysis bed temperature control

The control system managed the temperature within 25°C of the set point on CRIPS 1 using the speed of the auger to return the sand. CRIPS 1 was designed to utilise the NCG stream as the fluidisation medium for the pyrolysis reactor. The NCG produced by the pyrolyser was purged to the combustor to reduce the fuel load and to control the pressure in the freeboard of the PFB.

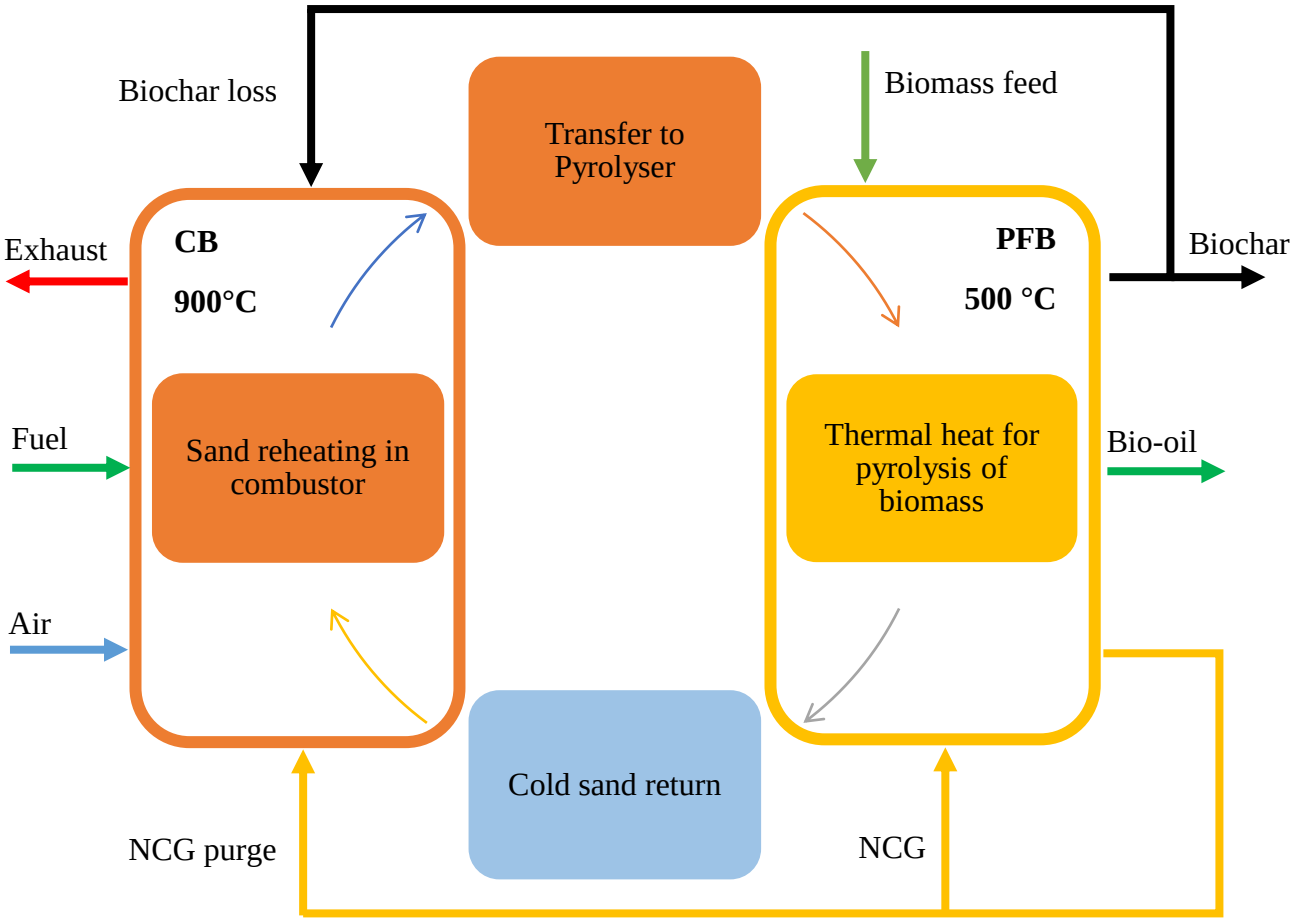

Figure 7: Dual bed CRIPS process with sand transfer

The biomass was fed pneumatically to the reactor using the NCG as a carrier gas. The feeder box received biomass from the hopper shown in Figure 9, which was fed via a speed-controlled auger. The NCG was injected from the top, blowing past the auger opening and exiting with the biomass via two pipes. This design resulted in blockages of the feeder box and the exit pipes due to the flow of gas being in the direction of gravity, which allowed the biomass to clump together and block the exit pipes.

A new design of this feeder was done with the NCG injected from below. This allowed the NCG to entrain biomass from the auger and exit via two pipes at the top. This was done to prevent gravity blockages. The feeder was 3D printed using ABS plastic to ensure that the new design was functional before constructing a unit from steel. The new design is shown in Figure 8.

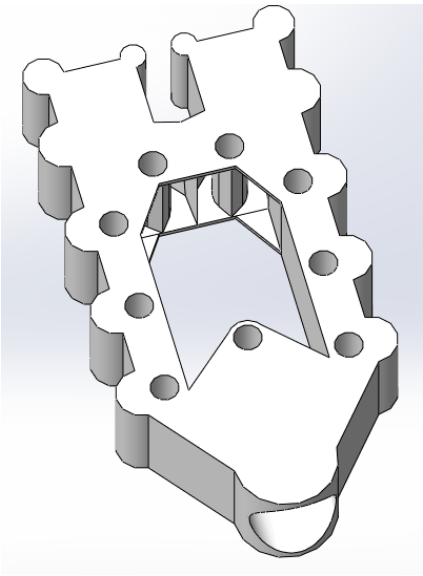

Figure 8: ABS model of feeder

Several units were printed using different plastics and techniques before one was fitted to the hopper. The unit is shown in Figure 9.

Figure 9: Feeder fitted on hopper

The unit features a viewing glass for visual inspection of biomass feeding. The design was expected to perform well; however, the decision was made to use mechanical feeding for CRIPS 2 because of problems with the gas flow required for successful biomass entrainment

and the subsequent increases in pressure drop. The biomass is fed via a drop pipe connected to the new reactor in CRIPS 2 by a fast-rotating auger.

The feeding system encounter problems with bridging and blocking in the hopper, so an agitator was fitted inside the hopper and driven via a chain-and-sprocket drive. The agitator is illustrated in Figure 10.

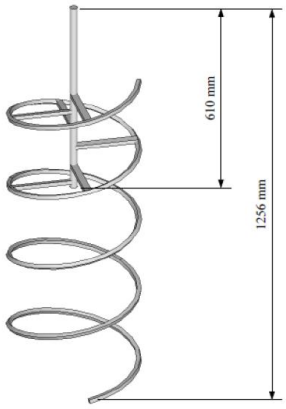

Figure 10: Hopper agitator design (Swart 2012)

The final agitator installed had a central shaft running down to the very end of the spiral. The spiral ended short of the opening to the auger because of the conical shape of the hopper. This allowed bridging to occur above the auger and interfered with the smooth feeding of biomass. To prevent this from occurring, a thin metal plate was welded to the shaft of the agitator, which extended the agitation to just above the auger and broke up any possible bridging.

The biomass is converted to NCG, bio-oil vapours and biochar, the yields of which will be discussed in Section 4. The biochar is a valuable product for use in forestry and agricultural land to replenish soil. CRIPS 1 however only recovered 58% of the biochar in the char cyclone after the PFB. The remainder is entrained via the sand returned to the CB and burnt for heat generation. The char is separated in the cyclone after which the vapours enter the quencher, where a spray of cooled bio-oil is used to condense and cool the mixture. The setup can be seen in Figure 11.

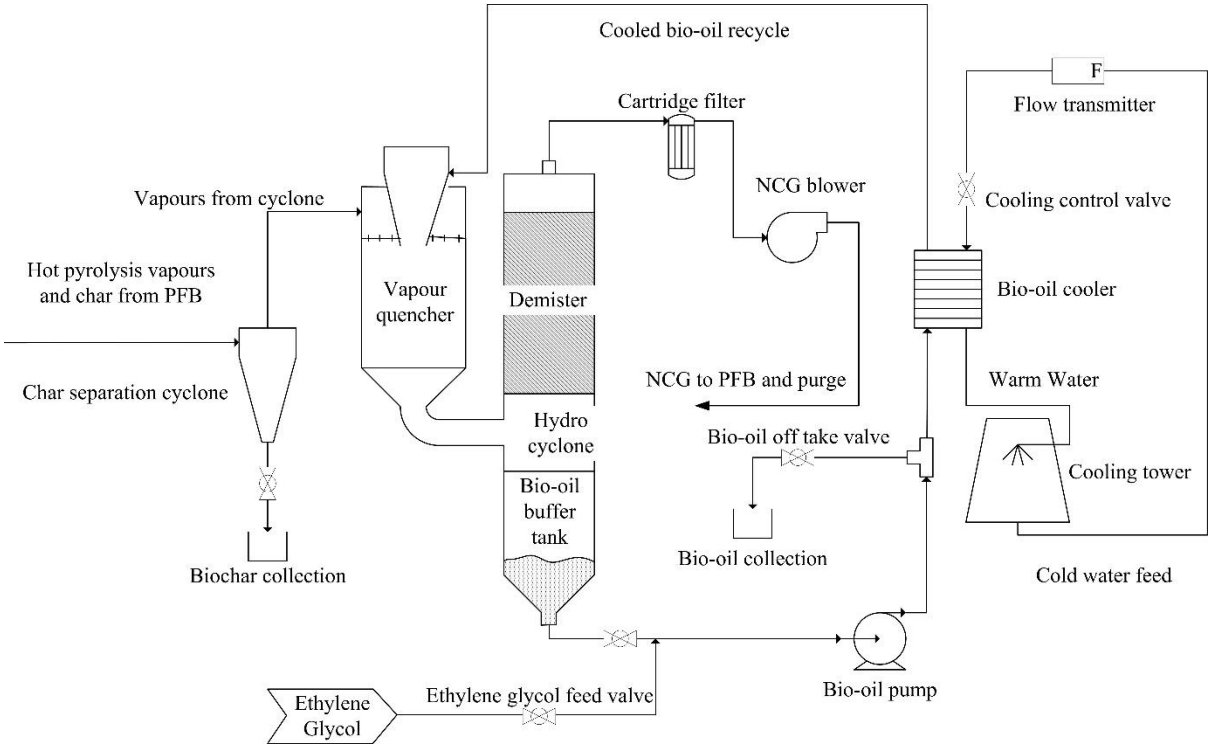

Figure 11: Product separation flow diagram

The quencher design in CRIPS 1 resulted in high pressure drops in the NCG loop because the pyrolysis vapours were used to atomise the cold bio-oil recycle. A new unit was designed for CRIPS 2. The unit uses a conical design to generate a conical spray of bio-oil through which the hot pyrolysis vapours is blown. This ensures adequate contact between the two and the total condensation of the bio-oil vapours.

The bio-oil and NCG mixture is then separated by a hydrocyclone. The bio-oil is collected in a reservoir and the NCG passed through a demister and filter to remove any remaining oil droplets. The NCG flows back to the NCG blower. After the blower a purge is sent to the CB for combustion and the remainder is used to fluidise the PFB. The actual process is shown in Figure 12.

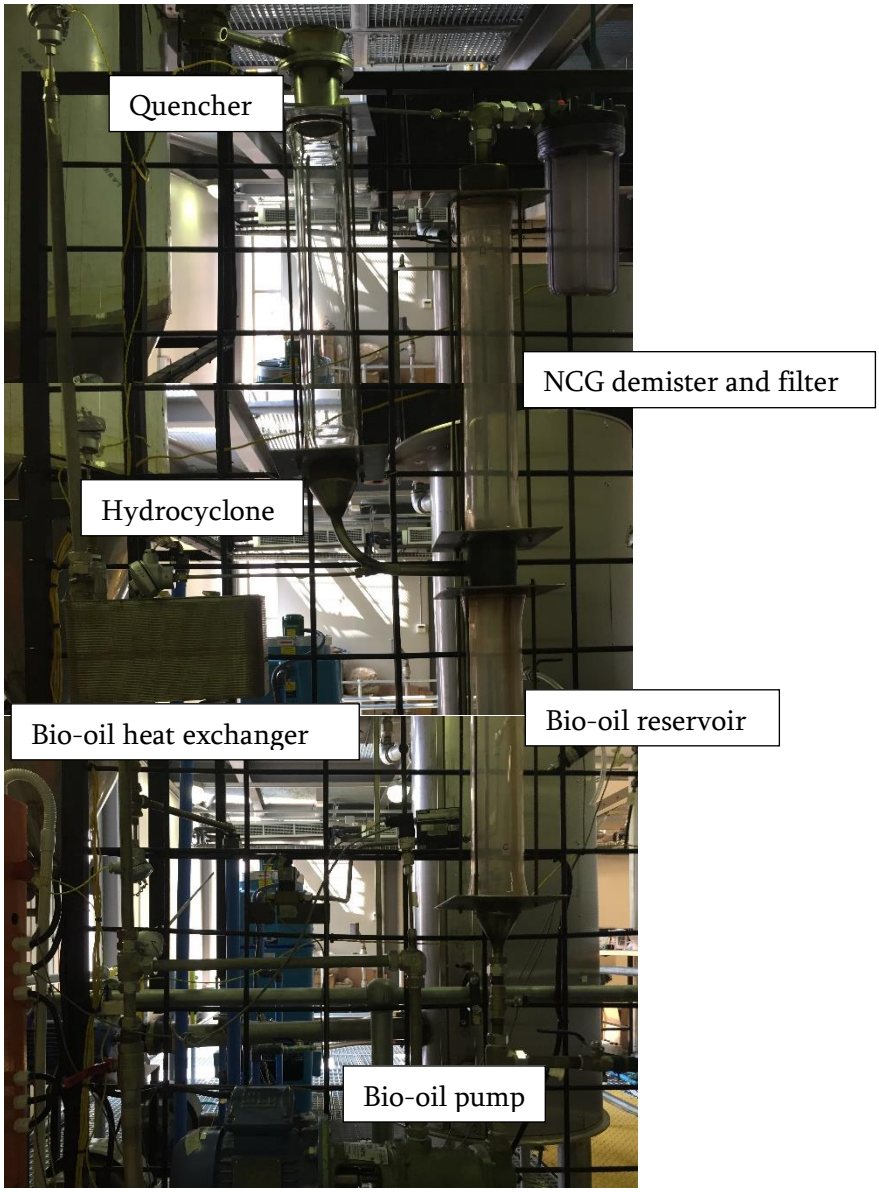

Figure 12: Product separation and cooling system

The bio-oil is pumped from the oil reservoir to a heat exchanger where it is cooled with cold water and fed back to the quencher. The cooling water is supplied by the cooling tower shown in Figure 13.

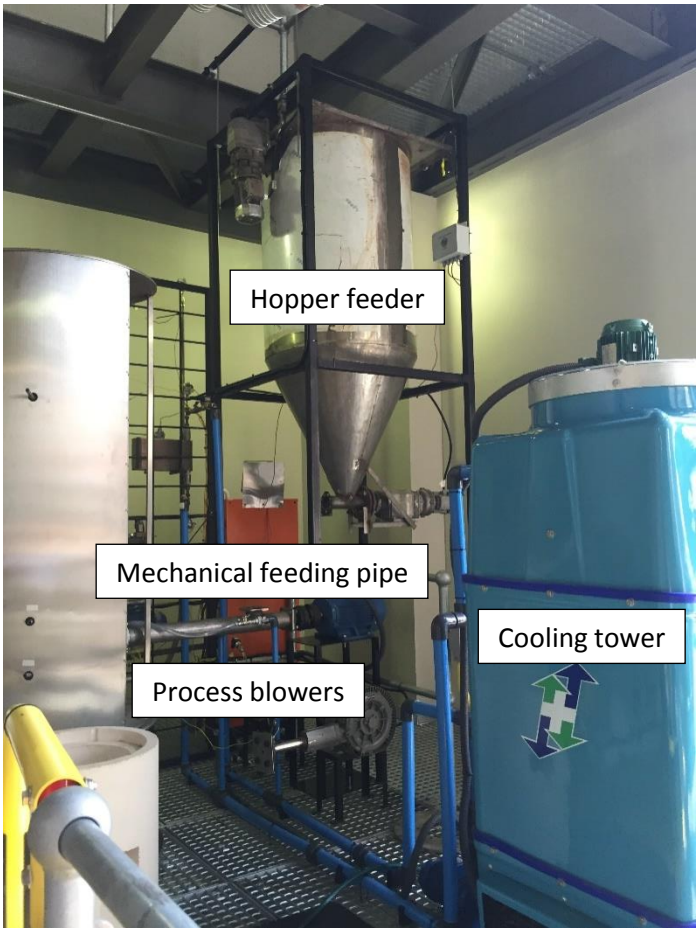

Figure 13: View of the process

4 CRIPS Process Modelling

The CB in CRIPS 1 built by Swart (2012) was supplied with cold air by a blower and used to fluidise the bed. The cold air feed required large amounts of heat to reach the 670 °C bed temperature. The planned bed temperature was 900 °C however the combustor was never capable of achieving this. This heat came from the combustion of LPG and electric elements. As a result less of the energy generated was left for pyrolysis, but due to heat losses this figure was lower. After combustion the exhaust gases flowed through a cyclone to remove entrained sand. The exhaust was then diluted and cooled by mixing with air and blown off.

CRIPS 1 was designed to pyrolise wood biomass at a rate of 20 kg/h; however, because of the heat and energy losses described above, the unit only managed 2,1 kg/h as reported by Grobler (2014). This was mainly due to the heat losses from the system and the problems with biomass feeding. These reasons, together with the conditions listed in the literature section, were used to set up an energy balance around the process. This energy balance formed the basis of the enthalpy balance approach to estimate bio-oil quality and yield, as well as process efficiencies.

The bio-oil, NCG and char yields (on a dry basis of *E. grandis*) were used as 36% bio-oil (including water), 14% NCG and 50% biochar as found in the process (Grobler 2014). This in agreement with ranges given in literature, however recent studies all suggest bio-oil yields of 65% to 75% when using fluidised bed fast pyrolysis (Amutio, et al. 2015). The reason for the low yield in bio-oil reported by Grobler (2014) is most likely due to the long vapour residence times reported with CRIPS 1, which exceeded 4 seconds during the experimental runs. This is double the recommended time of 2 seconds for fast pyrolysis (Bridgwater 2011). The increased residence time at temperatures above 150 °C promote char catalysed cracking of the vapours into smaller molecules and char.

The char extracted from the process was found to contain 54% inorganic material of which 42% was entrained sand from the bed and 12% was inorganics or ash from the wood. This

would imply that while 50% biochar was produced based on the dry wood feed only 29% was recovered via the cyclone and the remaining 21% was entrained and fed to the combustor. The high char yield will be discussed further on.

Since the NCG was used as the fluidisation medium for the pyrolysis bed, it was possible to use the 14% yield of NCG as a fuel source for pyrolysis. The NCG composition for the pyrolysis of *E. grandis* at 500 °C was specified as 45% CO_2, 25% CO, 16% CH_4 and 4% H_2, based on work done on similar fast pyrolysis systems (Heidari, et al. 2013). The balance was water vapour. This results in a CO/CO_2 ratio of 0,55 for CRIPS 1.

The air and NCG flow rates were determined by specifying the superficial gas velocity (SGV) together with the geometry of the CB and PFB. The CB SGV was set at 0,4 m/s because of the blower capability and the PFB SGV was set at 0,4 m/s because of the pressure drop on the cooling system. The air flow rate was used to determine the oxygen available for combustion based on 6% of the oxygen exiting with the exhaust, this was done to allow excess oxygen which would improve combustion completion. The reactor was modelled with LPG combustion to provide the heat for combustion.

To determine the flow of LPG, the oxygen consumed by the purged NCG and unrecovered char combustion had to be determined. The formation of NCG and char is reliant on the heat generated from combustion, and an iterative process was developed to converge on the LPG gas requirement based on the 6% oxygen less the NCG and char combustion. The LPG flows together with the NCG, and the char combustion was used to establish the total energy generated during combustion. The total energy generated, less the energy used to heat the air to 670 °C and the energy lost in heat loss, was assumed to flow to the pyrolysis reactor.

The total heat transferred to the pyrolysis reactor was needed to determine the biomass feed rate. This energy, less the energy used to heat the NCG and wood to 500 °C and the heat loss from the PFB, was available for pyrolysis. This, together with the experimentally determined heat of reaction for the pyrolysis of the wood, determined the biomass feed rate.

The heat of reaction was determined by Boateng using their experimental apparatus. A controlled amount of biomass was fed with nitrogen to an electrically heated fluidised bed after which all of the material was cooled and condensed, while the total heat load on the element and condenser was recorded. The CV of the biomass (*E. grandis)* was found to be 17,9 MJ/kg and the HHV of the resulting bio-oil as 17,4 MJ/kg. The data from the experiment is given in Table 2.

Table 2: Energy data from the Boateng study

Component	Internal energy (kJ/kg)	Mass (kg/h)	Heat added or removed (kW)	Physical properties used
		In		
Nitrogen	0	1,93	0	N/A
Biomass	17935	2,22	2,12	N/A
		Out		
Nitrogen	-	1,93	0,262	Enthalpy data
Bio-oil	18400	1,68	1,17	The condenser balance
Char	24850	0,22	0,031	Heat capacity
NCG	6230	0,31	0,2	Heat capacity
Heat loss	-	-	1,002	From the total balance

The heat of reaction ΔH_R was calculated (-545 kJ/kg biomass) as the difference between the heat of formation of the products and the heat of formation of the biomass feed, however this is relative to 25 °C. The heat of evaporation was calculated (1966 kJ/kg biomass) as the sum of the heat removed via cooling of the products (excluding nitrogen). The two were added and reported as 1421 kJ/kg biomass, as a heat of pyrolysis. The results from the energy balance analysis on CRIPS 1 is given in Table 3.

Table 3: Energy balance analysis for CRIPS 1

System Property	Description	Specified value	Calculated value
CB temperature	Operating temperature of the CB	670 °C	-
PFB temperature	Operating temperature of the PFB	500 °C	-
CB-SGV	Superficial gas velocity in the CB	0,4 m/s	-
PFB-SGV	Superficial gas velocity in the PFB	0,4 m/s	-
Air feed	Air to the CB at 670 °C	-	0,018 m^3/s
NCG feed	NCG to the PFB at 500 °C	-	0,004 m^3/s
O_2 in Exhaust	Oxygen unreacted (set point % of feed)	6%	-
LPG feed	LPG flow, based on available O_2 less NCG and char use	-	0,75 kg/h
Heat generated	Energy generated during combustion of LPG, char and NCG	-	15,17 kW
Heat input	Heating from elements	2 kW	
Air inlet temperature	Temperature of the air at the distributor	25 °C	-
Energy in flue	Energy in flue gas leaving the system	-	5,2 kW
Heat losses	Heat losses from the CB	4,9 kW	-
Sand heat transfer	Heat transfer to the PFB via fluidised sand	-	5,07 kW
Sand transfer rate	Rate at which 900 °C sand must flow to the PFB	-	81 kg/h
Total heat flux	Total heat flux to the PFB	-	5,07 kW
Heat used for NCG	Heat required to raise the NGC to the PFB temperature	-	1,54 kW
Heat loss from PFB	Heat loss from the PFB	2,7 kW	-
Pyrolysis heat	Total heat available for biomass pyrolysis	-	0,89 kW
Heat of pyrolysis	Energy required to pyrolyse wood biomass	-	1421 kJ/kg

System Property	Description	Specified value	Calculated value
Biomass feed	Total possible biomass feed rate based on energy available	-	2,1 kg/h
NCG production	NCG production rate based on literature	-	0,3 kg/h
Bio-oil production	Production rate of bio-oil	-	0,8 kg/h
Biochar production	Total char recovered	-	0,64 kg/h

The analysis of CRIPS 1 closely follow the available performance data of the system as described by Grobler (2014). The following performance indicators were defined to determine the efficiency of the process: the recovery efficiency ($\eta_{Recovery}$) is a representation of the energy recovered in the bio-oil and biochar as a percentage of the biomass energy content. The thermal efficiency ($\eta_{Thermal}$) is an indication of the reduction in the fuel load required to run the pyrolyser because of NCG and char combustion. The overall efficiency ($\eta_{Overall}$) is a measure to determine what percentage of the total energy entering the system, from both biomass feed and fuel feed, is recovered in the products. The percentage loss (η_{Loss}) is a representation of the energy lost via cooling of the pyrolysis vapours to extract the bio-oil product and NCG recycle to the blower as well as the energy lost in the exhaust gas and heat lost from the system.

Table 4: Performance indicators for enthalpy balance approach (refer to Figure 14)

Parameters	
$\Delta H_{Exhaust}$	Thermal energy lost in exhaust gas (kW)
$\Delta H_{Cooling}$	Thermal energy lost in cooling of bio-oil and NCG (kW)
ΔH_{Loss}	Thermal energy lost as heat losses (kW)
$\Delta H_{C,Total}$	Sum of heat generated by combustion of fuel, NCG and biochar (kW)
$\Delta H_{C,Fuel}$	Heat generated by combustion of fuel (kW)
$\Delta H_{R,P}$	Heat of reaction for pyrolysis (-545 kJ/kg)

Performance Indicator	Calculation method
$\eta_{Recovery}$	$\frac{Energy\ in\ Biochar\ (kW) + Energy\ in\ Bio\text{-}oil\ (kW)}{Energy\ in\ Biomass\ (kW)}\ x\ 100\%$
$\eta_{Thermal}$	$\frac{\Delta H_{C,Total} - \Delta H_{C,Fuel}}{\Delta H_{C,Total}}\ x\ 100\%$
$\eta_{Overall}$	$\frac{Energy\ in\ Biochar\ (kW) + Energy\ in\ Bio\text{-}oil\ (kW)}{\Delta H_{C,Total}}\ x\ 100\%$
η_{Loss}	$\frac{\Delta H_{Exhaust} + \Delta H_{Loss} + \Delta H_{Cooling}}{\Delta H_{C,Total} + \Delta H_{R,P}}\ x\ 100\%$

The enthalpy balance approach for CRIPS 1 is shown in Figure 14 with the indicators in the bottom left-hand corner. The analysis derived a bio-oil with an HHV of 14,2 MJ/kg, which is lower than the bio-oil HHV produced by similar fast pyrolysis systems, which are reported to have HHVs in the range of 17-23 MJ/kg (Bridgwater 2011), (Lehto, et al. 2014), (Bridgwater, Meier and Radlein 1999), (Zhang, et al. 2013). The theory of the CO reduction taking place can therefore not be confirmed or discarded based on this energy balance. The heating value derived during the analysis is in agreement with those found in similar processes.

CRIPS 1 showed poor performance with an overall efficiency of 33%, due to the high energy losses of 100%. The high energy loss is due to the heat loss (7,6 kW) and the high-quality energy lost in the flue gas (5,2 kW) The analysis showed poor recovery of the chemical energy from the wood in the product. This is mainly due to the over production of char and the subsequent entrainment of char to the CB. The entrainment of char did however contribute largely to the 24% reduction in the fuel load on the pyrolyser.

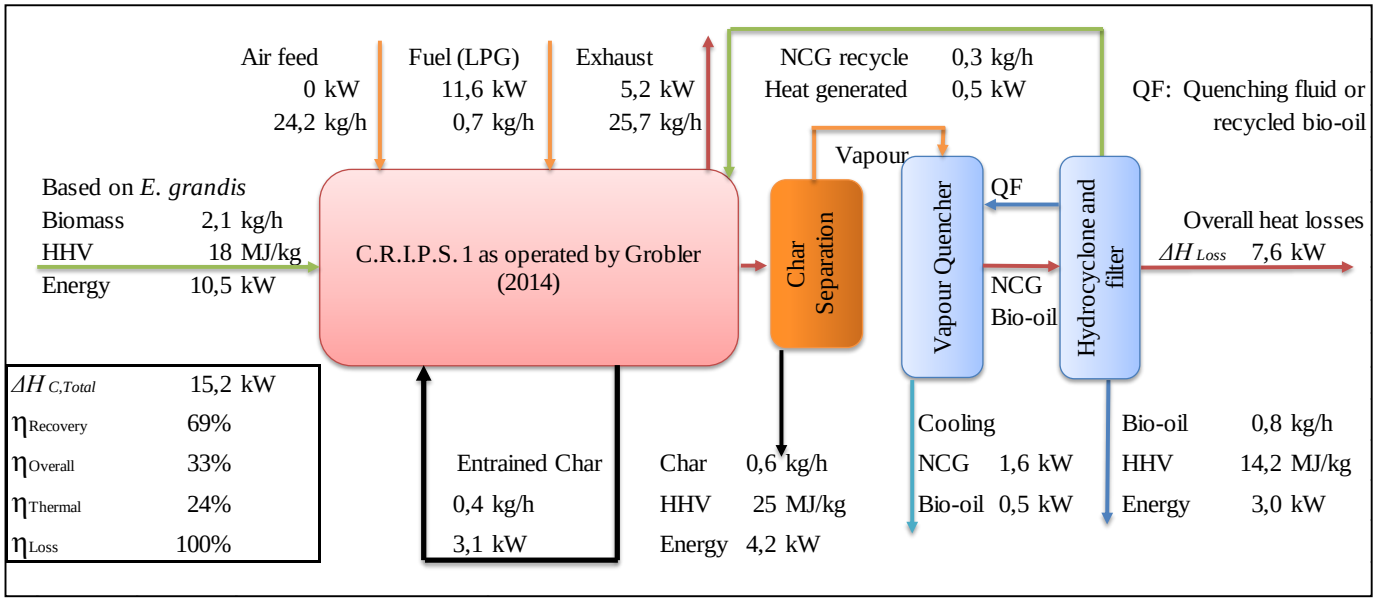

Figure 14: Enthalpy balance approach for CRIPS 1

The analysis did however show that the lower throughput of 2,1 kg/h was not due to high heat losses alone, the set points of the process for air flow to the combustor limited the quantity of biomass that could be processed even if all the energy was recovered from the flue gas or if the heat losses were eliminated. The CB was operated at 670 °C, although the aim was to operate at 900 °C to provide adequate temperature deference between the hot sand flowing to the PFB and the PFB temperature of 500 °C. The sand circulation rate was set at 81 kg/h with the 2,1 kg/h biomass feed. This is a ratio of 38 sand to wood.

A high CB temperature of 900 °C is recommended for the complete combustion of the fuel to carbon dioxide and water as well as the ability to design around 6% oxygen in the exhaust. The design will allow the use of high temperature sand in the PFB should it be necessary for high temperature pyrolysis bordering into gasification.

The energy lost via the exhaust gases and heat loss resulted in poor process efficiencies. It was therefore recommended to recover the energy lost in the exhaust gas by preheating the air feed to the reactor. The heat loss from CRIPS 1 should be limited by combining the high-temperature CB with the PFB, which operates at a lower temperature of 500 °C. The design of CRIPS 2 and the heat recovery are discussed in more detail in Chapters 5 and 6.

5 CRIPS 2 Reactor Design

The reactor design for CRIPS 2 was not done according to the conventional process such as the design procedure explained in Seider et al. (2010: 667), where the procedure is initialised by collecting kinetic and thermodynamic data on the desired reaction and possible side reactions, followed by physical data collection, modelling, testing and mechanical design. The reactor design was done based on the results of the energy model for CRIPS 1, together with the information gathered from the literature. This information was discussed in Chapter 2.

5.1 Principles and Design Considerations

A list of all considerations is given below. It was combined from the literature recommendations and the work done by Grobler (2014).

- PFB temperature of 500 °C with a CB temperature of 900 °C (Grobler 2014)
- Low residence time of vapours at high temperatures, typically less than 2 seconds
- Effective separation between char and sand – char must be entrained in vapours
- To this effect higher superficial gas velocities will be used in both the CB (more fuel) and the PFB (more char entrainment)
- The design allows for post-construction alterations to prevent unpredicted heat losses by combining both reactors into one unit – a CB inside an annular PFB

Further conditions are listed in both reports; however, these are the only conditions critical to the reactor design.

5.2 Reactor Design

5.2.1 Fluidised beds

The reactor design was based on the findings above that satisfy the greatest number of the considerations listed. Alternative designs were developed until the final design was set and approved for construction. The final design of the reactor features the combination of the CB into the PFB. The PFB therefore operates in an annulus around the outer wall of the CB. This limits the heat loss seen with CRIPS 1 since the 900 °C CB operates inside the PFB, and any heat loss is therefore into the pyrolyser.

The CB consists of three refractory cylinders stacked on top of one another. The bottom refractory was cast from a harder abrasion-resistant material since it will contain the fluidised bed. The two identical top refractories were cast from a softer, more heat-resistant material. This design allows any wall heat losses from the CB to pass into the PFB and be recovered. For control purposes the wall thickness of the refractories was increased to limit the heat transfer to the PFB via the wall since the PFB is controlled via the sand transfer rate.

Refractory materials were made up of Al_2O_3 and SiO with some other additives to give different properties. The aluminium oxide content contributed towards the abrasion resistance but offered less resistance to heat transfer. The silicon oxide content improves heat resistance but is a softer material. The balance between the two can deliver a product with the required strength and heat resistance.

The bottom refractory was cast from ACTlite HC, which is a harder refractory material containing more Al_3O_3 but still has sufficient heat-resistant properties. The unit is shown in Figure 15. It is 660 mm high with an inside diameter of 250 mm and an outside diameter of 390 mm. This resulted in a wall thickness of 70 mm, which is sufficient for limiting heat transfer. The fluidised bed operates inside this unit, and was planned to start 180 mm above the bottom up to a height of 580 mm, resulting in a bed height of 400 mm.

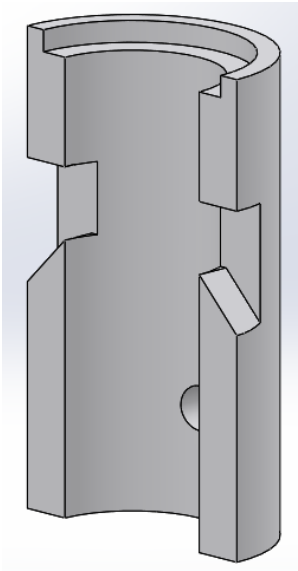

Figure 15: Bottom refractory

The unit features three holes for sand transfer. The two angled slots at the top are for 900°C sand to transfer to the PFB, which was expected to operate at a lower bed height of 300 mm. The bottom hole houses the auger in a pipe for the return of the 500 °C sand to the CB. The CB air inlet is located just below the bottom hole, which allows it to instantly fluidise the returning sand.

The sand used for the calculations has an average particle diameter of 0,8 mm in a range of 0,65 to 1 mm. The minimum fluidisation velocity of this material was calculated as 0,37 m/s with a bed load of 23 kg, yielding a bed voidage of 0,54. The bed will be operated at 3,2 times minimum fluidisation which ensures operation in the bubbling regime.

This process continues with an overflow of sand to the PFB because of the sand entering from below and raising the bed height. The top refractories were cast from ACTlite 40P, a material which is higher in SiO for better heat resistance. The units are both 500 mm high with the same diameters as the bottom unit. The units all feature a key at the top and bottom, which allows easy placement of the units on top of one another.

The CB uses LPG, the NCG purge and the entrained char to maintain the bed temperature of 900 °C, fluidising at a superficial gas velocity (SGV) of 1,2 m/s. This was specified to limit entrainment of the sand in the flue gas, while operating the blower at 70% capacity. The

freeboard above the bed was originally designed to ensure sufficient height for the return of entrained sand. It was, however, later decided to fit an internal heat recovery unit inside the freeboard for the sake of convenience and other reasons discussed in Chapter 6.

The PFB operates in an annular space around the CB. It features a 1,5 mm stainless steel outer shell, which also acts as the outer shell of the entire reactor. The reactor has a gas-tight seal between the shell, the heat recovery unit described in Chapter 6 and the PFB gas distributor described below.

The annular space surrounding the CB was designed to be 35 mm in diameter, but due to this narrow space and the recommended fluidised bed height-to-bed diameter ratio (L/D of 1), the 300 mm bed of the PFB was not practical. The bed height was specified to allow adequate contact time between the biomass particles and the heat carrier or sand.

The contact time was not calculated due to limited data with the fluidisation hydrodynamics of this kind of bed. If the bed is operated at a shallow depth the biomass conversion will be incomplete, however, CRIPS 1 was operated with a 200 mm bed depth and achieved complete biomass conversion and therefore it is assumed the 300 mm bed height will be sufficient. The need for complete contact between the biomass particles and hot sand requires a high degree of mixing inside the PFB. Since the sand overflow from the CB was limited to two places, a swirling or rotating bed of material was required in the PFB.

Studies done on fluidisation in an annular space with swirling beds found that large volumes of gas are needed to achieve full bed fluidisation and rotation or swirling (Batcha, et al. 2013). A minimum SGV of 10 m/s was required to achieve fluidisation with tangential or swirling velocities of 30 m/s required to achieve full bed rotation. These studies were modelled based on a system with a series of blades surrounding a cone in the centre, as shown in Figure 16.

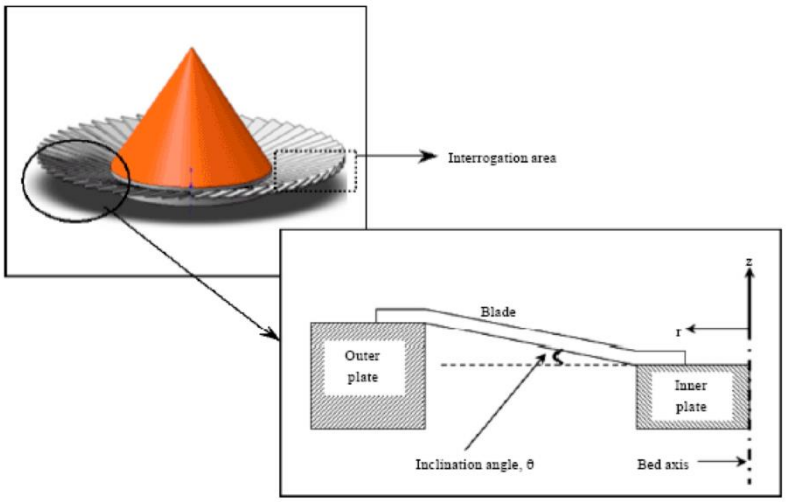

Figure 16: Distributor design (Batcha, et al. 2013).

The high volumetric flow rates required to deliver a SGV of 10 m/s would render the CRIPS process thermally insufficient, since the recycled NCG used to fluidise the PFB requires heating to 500 °C.

Further studies on the hydrodynamics of fluidisation in an annular space using various gas distributor designs illustrated the difficulty of fluidisation in an annular space (Wanicka and Heydenrych 2014). The limited gas flow set by the process conditions and difficulties found in other studies made it difficult to design the gas distributor for the PFB. A conical bed design was finally adopted similar to the conical bladed design in Figure 16.

The conical design allows the use of a narrower bed (10 mm gap) at the distributor level which is gradually increased in width to the 35 mm gap mentioned above. The narrower bed results in higher SVG velocities at the distributor level, ensuring full fluidisation using less volumetric flow. The expanding gap allows the disengagement of the fluidised particles above the bed. The design is shown in Figure 17.

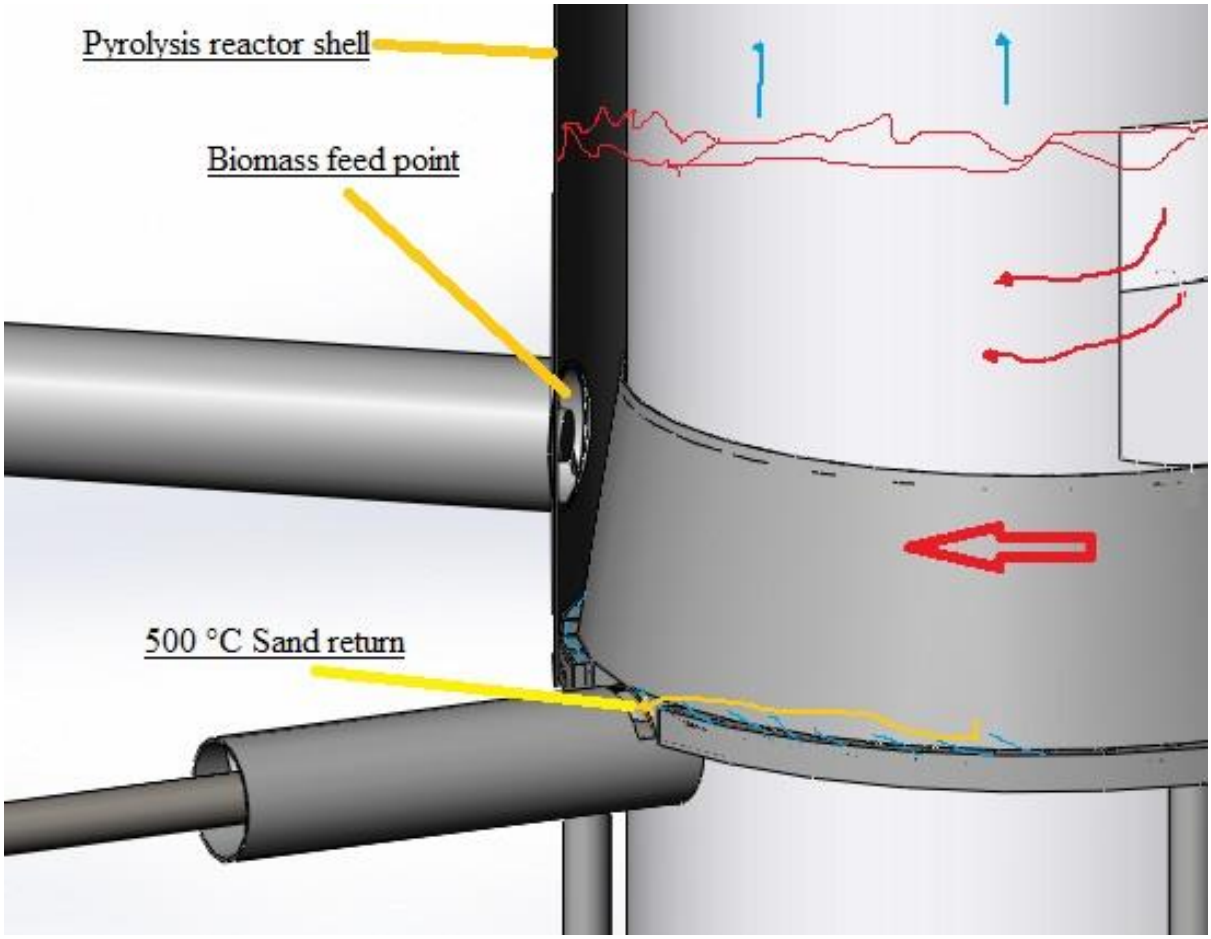

Figure 17: Pyrolysis gas distributor

The PFB has a vertical SGV of 3 m/s at the beginning, dropping down to 0,91 m/s at the full 35 mm width of the annulus. The SGV is much lower than that recommended by previous studies, but the CRIPS process cannot sustain a 10 m/s SGV with a 10 mm annulus, and a gap narrower than 10 mm would not be feasible for construction. The SGV should be sufficient since the PFB is not seen as a fully fluidised bed with normal densities. It is supplied by the CB with sand and is therefore only a fast-moving bed of material. The load of sand has been calculated as 8,2 kg in the annulus which yields a bed voidage of 0,77, higher than normally operated but necessary for the feasibility of this design.

The direction of the rotation is shown by the red arrow. Hot 900 °C flows from the CB via the angled slots based on the rate of sand returned via the sand auger (flow shown in orange).

The blue streamlines at the bottom show the jets created by the distributor. The red bubbling line indicates the planned bed height of 300 mm. The biomass is fed into the bed at one point by the biomass auger. It is injected 100 mm above the sand return point and 22,5° downstream. This was done to allow the biomass a full rotation of the bed before sand is withdrawn. The biomass with a lower density (160 kg/m^3) than the sand (1100 kg/m^3 fluidised) will float to the top of the bed and this should in theory prevent biomass from being transferred to the CB.

Modelling of the design was done in COMSOL Multiphysics© software and it was found that with a SGV of 3 m/s a tangential velocity of 25 m/s could be attained. This tangential velocity was found using a blade angle of 12°, which is in agreement with previous studies. The number of blades was adjusted to ensure a jet velocity of 50 m/s at the blade exit. This velocity reduces the chance of a section of bed becoming unfluidised because the jet is blocked.

The design was finally checked using 3D printed scale models of a 35 mm distributor with no cone and a 10 mm distributor with a cone, correctly scaled. The 10 mm gap required substantially less air to fluidise and rotate a bed of materials than the 35 mm gap version.

The distributor and cone were welded to four 20 mm instrumentation tubes which were welded to the base plate. The use of four feeding pipelines ensures equal distribution of NCG to all blades.

5.2.2 Heat loss estimation

The placement of the CB inside the PFB is the first step in limiting heat loss since it prevents heat loss from the 900 °C CB to the ambient conditions outside the reactor. The outer shell of the PFB is therefore the next major area for heat loss and for this reason it was insulated with 50 mm of high-temperature insulation followed by 75 mm of lower-temperature, high heat-resistant insulation to limit heat loss to a minimum and thereby preventing the heat loss experienced by CRIPS 1.

The insulation layers were modelled with conductive and convective heat transfer to determine the heat loss between the 500 °C outer shell and the ambient temperature. A variety of materials were modelled and the minimum heat loss was determined to be 1,19 kW. The PFB shell is, however, not the only area of concern for heat loss, since the CB top and bottom plates are still exposed to ambient temperatures. The heat loss from this section was estimated to be 2 kW due to the low area for heat transfer.

The heat transferred via the CB refractory wall was calculated to be 2,7 kW, which will be required for the energy balance in Section 7.

5.3 Conclusions and Recommendations

The reactor designed for CRIPS 2 eliminates many of the problems experienced with CRIPS 1, including heat loss and biomass feeding problems. The design had some difficulties of its own with the successful fluidisation of the PFB. The expected performance is detailed in Chapter 7 by the analysis of the energy balance. The use of blades around a conical design pose a potential problem for larger reactors since the 10 mm gap will be increased, however, larger designs could incorporate the preheating of the NCG feed, which would increase the volumetric flow through the jets and the annulus. The feasibility should be considered based on the actual results of CRIPS 2.

With increases in the gap width at the bottom, the radial distribution of the SGV and tangential velocities become uneven and could lead to fluidisation problems along the length of the blades. It is recommended that the blades be inclined from the cone outward towards the shell (Figure 16). This incline forces the equal distribution of SGV and tangential velocities and significantly reduces the pressure drop over the distributor (Batcha, et al. 2013). Please note a technical drawing is given in Appendix C.

6 Internal Heat Recovery Unit

The CB typically operates at 900 °C to provide a temperature difference of 400 °C between the PFB and the CB. This temperature is usually maintained by the combustion of gas (LPG) or solid (biomass, coal) fuels. Typically 35% of the heat generated in the CB is transferred to the PFB via sand transfer, with 56% lost in the heating of the exhaust gas, leaving the system at 900 °C. The remaining heat is assumed to be lost.

Grobler (2014) suggested using the energy in the exhaust gas to preheat the combustion air feed and thereby re-using the heat inside the reactor and increasing the heat transfer to the PFB. This ultimately increases the throughput of the reactor. It was also suggested using the flue for preheating the NCG recycle to the PFB or to dry the biomass. The problem with this is the varying composition of the NCG, and preheating it with 900 °C flue gas could cause an unwanted reaction. The use of the exhaust for drying at that temperature would cause the same problems with the wood.

The most feasible option is therefore to use the flue to preheat the air feed in a gas-to-air heat exchanger, possibly followed by using the colder flue gas for drying. Before a design can be done the feasibility of using high-temperature gas must be considered.

The temperature of the flue gas is too high for conventional gas heat exchangers. It can cause corrosion problems which could lead to failure. Cooling the flue gas below 300 °C is not recommended since it can lead to condensation of corrosive components (Seider, et al. 2010). For the heat recovery to be financially feasible the air feed should be heated above 400 °C and this is typically only done in a furnace.

The materials needed for such a construction would make the manufacture and maintenance of the unit difficult and expensive since stainless steel has a maximum service temperature of 700 °C.

Considering all of these factors and limitations, a new design was done in which the space above the CB known as the freeboard was used for the insertion of an internal heat recovery (IHR) unit. The design is similar to a shell-and-tube heat exchanger, the difference being

that the tubes are spaced around a central pipe in an annulus. An early design is shown in Figure 18.

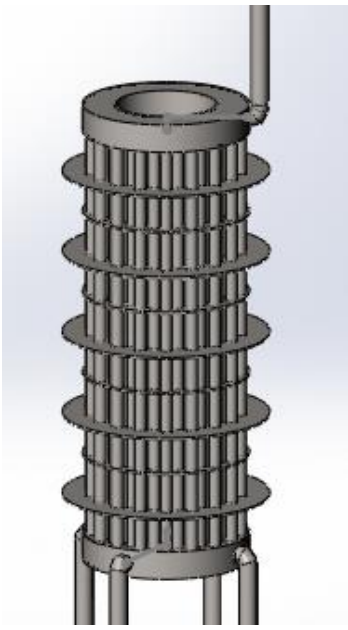

Figure 18: Internal heat recovery unit

This design allows a central cavity to remain open which can be used for visual access to the CB or to feed solid fuels. The baffles are made of interchangeable steel disks called doughnuts and rings (Sinnott and Towler 2010). The flue gas is channelled around the outside of the tubes with the fresh air feed inside the tubes.

The design of the heat recovery unit was based on the geometry of the CB and viewing hole. The internal CB diameter of 250 mm and the 90 mm viewing shaft required in the centre put severe limitations on possible designs. The first design consisted of bending five tubes in a spiral around the central pipe. This would allow the flue gas to flow up in a staggered pattern across the tubes. This design was modelled and ultimately resulted in linear gas velocities of 170 m/s.

These velocities were the result of the 500 °C plus the final air temperature combined with the limited five-pipe design, which resulted in very high volumetric flow rates per pipe. The high velocities would cause significant pressure drops and cause vibration problems in the unit. The design was altered to that of the earlier unit shown in Figure 18. The number

of tubes were increased to 48, allowing lower volumetric flow rates per tube. The tubes were arranged in such a way as to provide staggered horizontal flow across the tubes.

This resulted in maximum final outlet tube velocities of 10,5 m/s, which was not a concern for pressure drop. The design of the unit was based on the design for a shell-and-tube heat exchanger, where the external forced convection method is used to calculate the shell side heat transfer coefficient and the internal forced convection method is used to calculate the tube side heat transfer coefficient (Cengel and Ghajar 2011).

The two heat transfer coefficients are combined as total heat transfer resistances and converted to an overall heat transfer coefficient. This overall heat transfer coefficient was used with Equation 1 derived from the log mean temperature difference to determine the exit temperature T_e of the air.

$$T_e = T_s - (T_s - T_i)e^{\left(-\frac{A_S U}{mC_p}\right)} \tag{1}$$

T_i is the inlet temperature of the air and T_s is the bulk mean temperature of the flue gas seen as the surface temperature. A_s, C_p and m refer to the area for heat exchange, the heat capacity of air and the mass flow of the air respectively. Once the outlet temperature of the air was known, the log mean temperature was calculated and the heat transfer determined. Once the heat transfer was known, the exit temperature of the flue gas could be calculated.

Since the outlet temperature of the flue gas was required to determine the bulk mean or surface temperature, an initial value was guessed and then an iterative calculation was done until the bulk mean temperature converged.

The properties of both the air and the flue gas differ significantly over the temperature range observed for this heat exchanger. For this reason the unit was broken up into 13 sections. Each section represents the space between baffles. The design is shown in Figure 19.

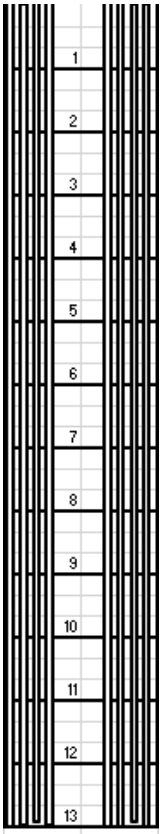

Figure 19: Sectional design of heat exchanger

The properties of the air and the flue gas were determined for each section using the bulk mean temperature of each material for that section. The outlet temperature of a previous section was used as the inlet temperature of the next section and so on. The heat exchanger inlet and outlet temperatures for each baffle are shown in Figure 20.

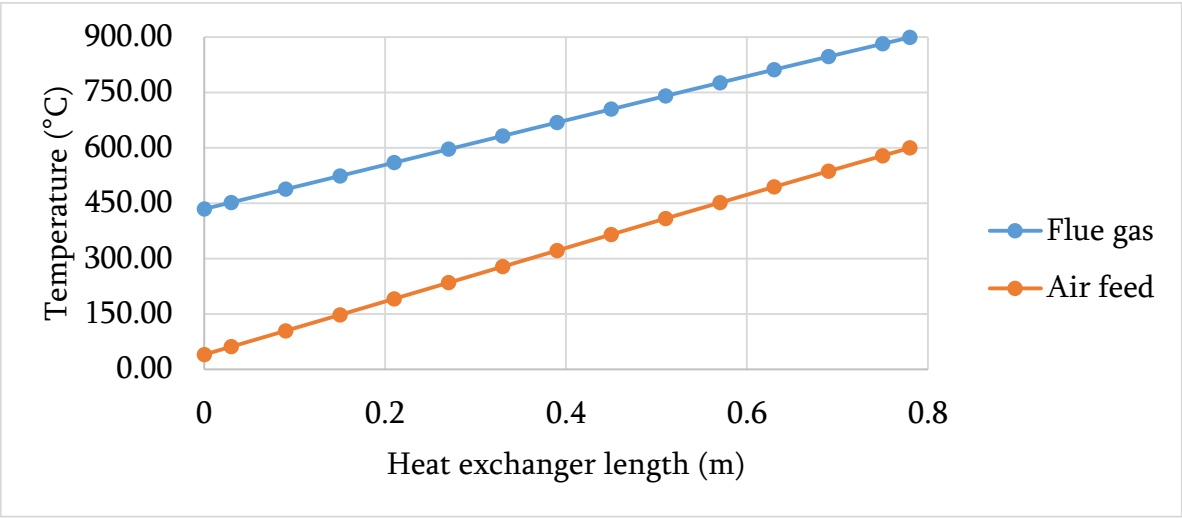

Figure 20: Heat exchange profile

The inlet and outlet temperatures in Figure 20 lie at the extremes. The data points between these temperatures represent the bulk mean temperature of each material in the individual sections. The unit maintains a minimum temperature difference driving force of 300 °C, which is well above the recommended minimum of 150 °C (Seider, et al. 2010). The design meets all the requirements set above, including placing the unit in a furnace since the combustor can be viewed as a furnace above the CB.

The flue gas leaves the system at 433 °C, well above the temperature for any risk of condensation, and still contains sufficient energy for drying purposes as suggested by Grobler (2014). The total heat transferred by the unit was modelled as 10,7 kW with a total surface area of 1,18 m^2. The overall log mean temperature difference is 334 °C, with an average overall heat transfer coefficient of 26,4 W/m^2C. This overall heat transfer coefficient is in accordance with values suggested by the literature (Seider, et al. 2010). The unit has the potential of reducing the heat lost in the exhaust gases by 54%.

The mechanical design of the heat exchanger proved difficult because of the confined space of the CB. The design was altered several times after the input from a possible manufacturer. The IHR unit is shown in Figure 21.

Figure 21: Final heat exchanger design

The unit features a wide-diameter plate at the top into which the tubes are welded. It also serves as the lid for the entire reactor and is bolted to the PFB shell. The air distributor is constructed of a top disc and shell, which can be seen at the very top. It was designed to provide good distribution of the air and also to insulate the CB radiation from the environment.

The bottom of the unit contains the air collection point. This is where the air flows recombine and exit the unit via four pipes. The number of pipes were selected based on minimising the pressure drop while maintaining ease of construction. The exhaust gas flow can be seen in Figure 22.

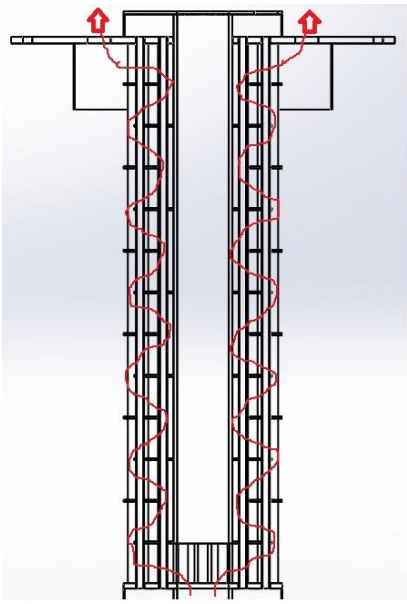

Figure 22: Sectional view with exhaust flow

The flue gas enters the unit on the inside of the annular tube bank and flows across the tubes and up into the second section. This flow continues around the entire unit until the gas reaches the last baffle. At the top the flue gas makes a final pass across the tubes before extraction from the reactor.

7 CRIPS 2 Process Modelling

The design for CRIPS 2 was used together with the operating principles described in Chapter 4 to create an energy model for CRIPS 2. The energy balance and mass balance are shown in Table 5.

Table 5: System set points and operating conditions

System Property	Description	Specified value	Calculated value
CB temperature	Operating temperature of the CB	900 °C	-
PFB temperature	Operating temperature of the PFB	500 °C	-
CB-SGV	Superficial gas velocity in the CB	1,2 m/s	-
PFB-SGV	Superficial gas velocity in the PFB	0,91 m/s	-
Air feed	Air to the CB at 900 °C	-	0,059 m^3/s
NCG feed	NCG to the PFB at 500 °C	-	0,042 m^3/s
O_2 in Exhaust	Oxygen unreacted (set point % of feed)	6%	-
LPG feed	LPG flow, based on available O_2 less NCG and char use	-	1,94 kg/h
Heat generated	Energy generated during combustion of LPG, char and NCG	-	37,7 kW
Air inlet temperature	Temperature of the air at the distributor	-	600 °C
Energy in flue	Remaining energy in flue gas leaving the system	-	9,66 kW
Heat losses	Estimated heat losses from the CB	2 kW	-
Wall heat transfer	Heat transferred to the PFB via the refractory wall	-	2,72 kW
Sand heat transfer	Controlled heat transfer to the PFB via fluidised sand	-	23,3 kW
Sand transfer rate	Rate at which 900 °C sand must flow to the PFB	-	158 kg/h
Total heat flux	Total heat flux to the PFB	-	26,0 kW

System Property	Description	Specified value	Calculated value
Heat used for NCG	Heat required to raise the NGC to the PFB temperature	-	14,5 kW
Heat loss from PFB	Heat loss from the PFB	-	1,19 kW
Pyrolysis heat	Total heat available for biomass pyrolysis	-	10,3 kW
Heat of pyrolysis	Energy required to pyrolyse wood biomass	-	1421 kJ/kg
Biomass feed	Total possible biomass feed rate based on energy available	-	26,1 kg/h
NCG production	NCG production rate based on literature	-	5,2 kg/h
Bio-oil production	Production rate of bio-oil	-	16,2 kg/h
Biochar production	Total char recovered	-	4,2 kg/h

The expected performance of the system is to pyrolyse 26,1 kg/h of wood biomass using 1,94 kg/h of LPG. The process will produce 16,2 kg/h of low-quality bio-oil. The LPG usage was reduced by 34% because of the NCG purge and char loss to the CB. The CO/CO_2 ratio used was kept at 0,55 which is in agreement with similar pyrolysis processes (Amutio, et al. 2015).

The addition of the heat recovery unit, which preheats the air feed to 600 °C by recovering 10,7 kW of heat from the flue gas, resulted in an increase in the throughput of the reactor. This results in a vastly more efficient system compared to the previous process.

8 CRIPS 2 Performance Evaluation

The energy balance combined with mass balance given in Chapter 7 is accurate enough to suggest its use as a tool for the determination of bio-oil heating value and yield. The enthalpy balance approach was defined and used to compare the efficiencies of different processes. Performance indicators were defined to determine the performance and efficiency of a process – they are defined in Table 4 (page 28).

CRIPS 2 was designed to solve the problems of CRIPS 1 by limiting energy losses and improving sand transfer. For this reason the CB was placed inside the PFB, thereby causing any heat loss from the 900 °C CB to transfer into the PFB. The PFB was then insulated by 125 mm of high-temperature insulation to limit losses from the 500 °C zone.

The gas flow rates required to fluidise the PFB require heating to 500°C, and the energy used via this process can be seen in the enthalpy balance for CRIPS 2 (Table 5). The design of the internal heat recovery unit (IHR) was based on the principles of a shell-and-tube heat exchanger to utilise the area in the combustor above the bed. The IHR recovers energy from the 900 °C flue gases by exchanging heat between the exhaust gases and the fresh air feed to the combustor. By doing so all heat lost from the IHR remains inside the reactor and improves the efficiency of the process. The enthalpy balance approach for CRIPS 2 is shown in Figure 23.

The yields of bio-oil, NCG and biochar were specified as 62% bio-oil (Amutio, et al. 2015), 20% NCG and 18% biochar (Bridgwater 2011), which is in agreement with similar processes. This assumption was made because of the vapour residence time and pyrolysis temperatures.

The recovery efficiency has improved to 89% compared to the 69% seen earlier, mainly because of the recovery of more char via the cyclone. The thermal efficiency of the process remains the same, with a 34% reduction in the fuel required to pyrolise the increased throughput. The rise in the overall efficiency is due to the significant drop in energy losses from the system.

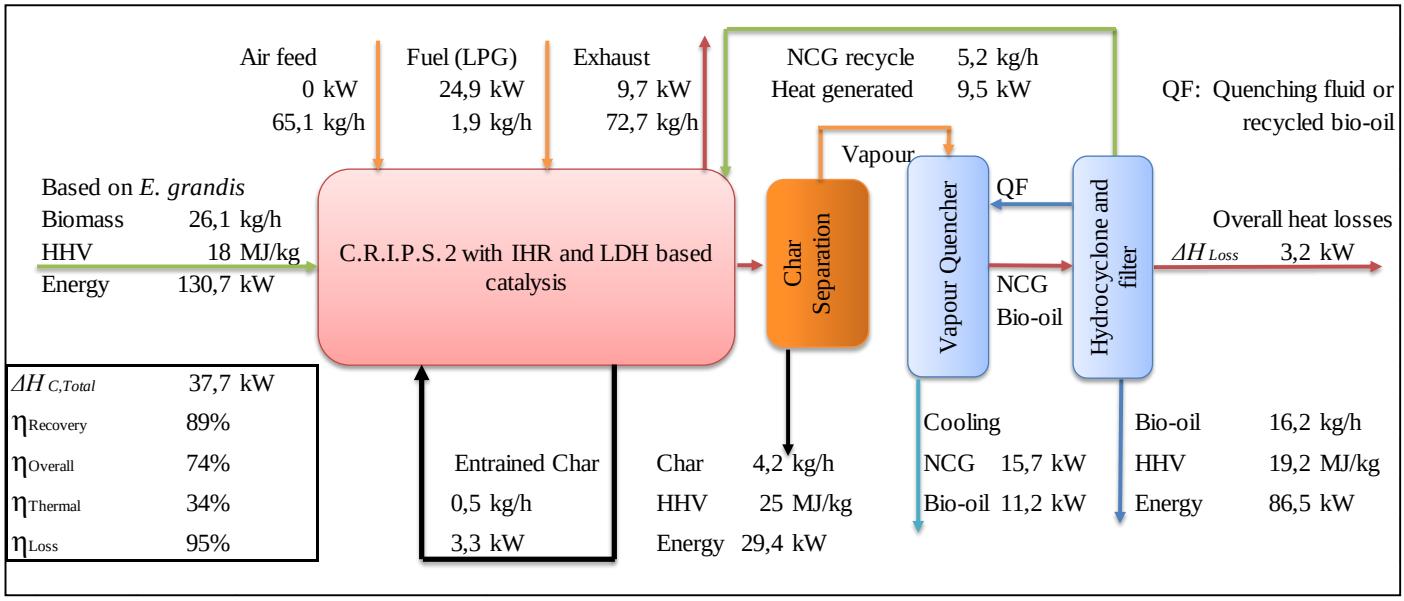

Figure 23: Enthalpy balance approach for CRIPS 2

The bio-oil derived for CRIPS 2 has a higher HHV of 19,2 MJ/kg compared to that of CRIPS 1 of 14,2 MJ/kg. This is plausible since the analysis above was done for a process with vapour residence times of 1,3 seconds, which would reduce the cracking of the oil vapours into small non condensable gasses, thereby adding to the heating value of the oil. The heating value of the oil is derived as the unknown in the energy balance since the other energy flows and mass flows are known. The balance is done and the mass flow of the oil is used to report the energy content of the oil as an HHV.

The use of the internal heat recovery unit is expected to greatly improve the efficiency and throughput of the CRIPS process, however the exhaust gas still contains a recoverable 3,3 kW of thermal energy before the 300 °C lower limit for flue gas is violated. This energy could be used to preheat the NCG feed to the PFB and reduce the heat load in the PFB to 11,2 kW, which would increase the biomass throughput of the process by 8,4 kg/h. The NCG volumetric flow would also increase and as a result the jet velocities would increase by 25% which would aid in the operation of the PFB distributor.

9 CRIPS 2 with Catalytic Pyrolysis

The analysis of the CRIPS 2 enthalpy balance and the expected results merit consideration for the in situ catalytic upgrading of the bio-oil. The use of bentonite and zeolite catalysts has proved effective in upgrading the oil (Merckel and Heydenrych 2015); however, due to the nature of these catalysts, the oxygen in the oil is removed as water. This causes a drop in the H/C ratio and also promotes coking of the catalyst.

Alternatively, the metal oxides (MO) in LDH-based (layered double hydroxide) catalysts or metal sulphide (MS) catalysts can be used to upgrade the oil. The catalyst reacts with the bio-oil vapours, removing oxygenates and increasing the HHV of the oil. The catalyst, which is coked up and saturated with oxygen, requires regeneration in a high-temperature environment.

The catalyst can be regenerated and decoked by the high-temperature conditions in the CB. Since the catalyst must flow continuously between the CB and PFB to be effective, it can also be used to transfer the thermal heat required for pyrolysis.

The chemical looping process between the PFB and CB performs a triple function, including transferring the heat required for pyrolysis, upgrading the bio-oil vapours and decoking the catalyst. The catalyst transfer rate between the CB and PFB can be regulated by using the auger speed, allowing careful control of the pyrolysis bed temperature as shown in Figure 6 (page17) and the upgrading of the bio-oil vapours. This process is illustrated in Figure 24.

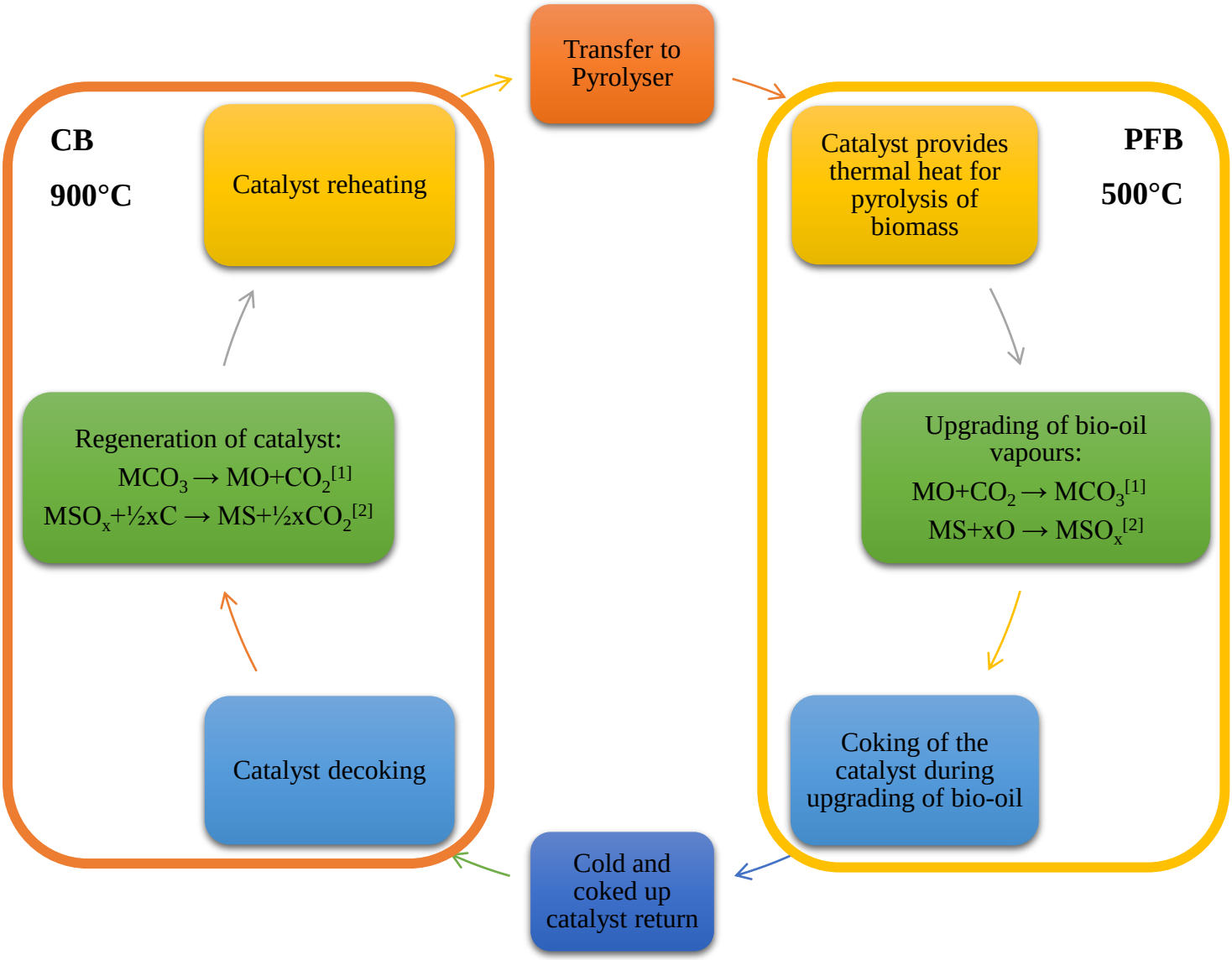

Figure 24: CRIPS 2 with triple function chemical looping

The MO captures oxygen in the form of CO_2 to become MCO_3, a decarboxylation reaction. The MCO_3 is then regenerated to MO in the combustor by the burn-off of the CO_2 group. The catalyst removes oxygen with a loss in carbon which increases the H/C ratio of the fuel, while reducing the O/C ratio. Alternatively, metal sulphide (MS) can be used as the heat carrier and catalyst. The MS removes oxygen from the bio-oil and forms sodium sulphate (Na_2SO_4). The sulphate can be regenerated with the use of free carbon in the CB. The biochar fraction lost in the circulating bed medium is a potential source of free carbon. The oxygen is burnt off as CO_2.

The combination of catalytic upgrading and pyrolysis in one reactor improves the effectiveness of the process and substantially reduces the need for downstream upgrading, which can often be expensive and energy intensive. Oil upgrading needs hydrogenation and hydrogen is expensive to produce (Sharifzadeh, et al. 2015).

It is immaterial which catalyst is used from an enthalpy balance point of view because the net result is the removal of oxygenates from the bio-oil as CO_2, which is burnt off in the CB. Recent work with LDH-based catalysts using analytical equipment produced a bio-oil with an HHV of 40,2 MJ/kg. This value was approximated using a cumulative H, C and O elemental analysis of the identified components in the oil. The H/C ratio was 1,56 and the O/C ratio was 0,076. The experimental work did not report NCG or char yields.

The active catalyst present in the PFB will upgrade the bio-oil vapours by the removal of oxygen as CO_2, bound to the catalyst in a carbonate group. It is assumed that due to the reactive nature of CO and the presence of the active catalyst that the CO produced during the initial pyrolysis of biomass would be converted to CO_2. This would cause the CO/CO_2 ratio to drop to near 0 and for the analysis given below it is assumed to be 0.

The water of pyrolysis, char and NCG yields were assumed to remain the same as for non-catalytic pyrolysis, which is reasonable considering that the upgrading mechanism is decarboxylation and this would not affect these yields. Only the composition of the NCG would change with the conversion of the 25% CO into CO_2.

The enthalpy balance approach for a CRIPS 2 process was used to analyse the potential oil yield and process efficiencies if an oil with an HHV of 40,2 MJ/kg is produced. An elemental balance was added to the mass balance component to account for the carbon and oxygen lost to the CB via the bound CO_2 in the catalyst. The complete enthalpy balance using a MO catalyst is shown in Figure 25.

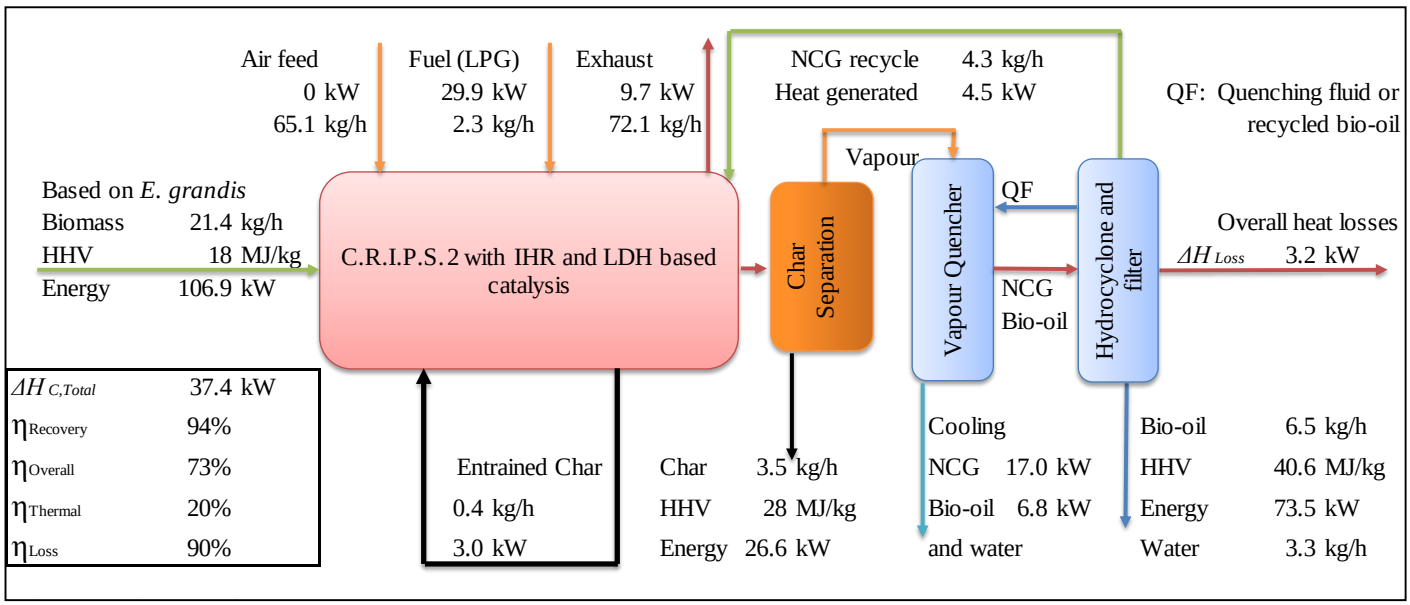

Figure 25: CRIPS 2 enthalpy balance approach with catalytic pyrolysis

The analysis of CRIPS 2 with in situ catalytic upgrading derived an HHV for the bio-oil of 40,6 MJ/kg, which is in agreement with the value reported from the experimental study. This would suggest that the assumption of the CO/CO_2 ratio reducing to 0 and the water, NCG and char yields remaining constant is feasible. The bio-oil yield for the analysis was 30,5% with the formation of 20% NCG, 18% char, 15,5% water and 16% CO_2 removed by the catalyst. All are reported on a dry basis of biomass.

The recovery efficiency of the process was improved by 5%, due to the increased HHV of the oil and the loss of only 50,8% in bio-oil yield. The overall efficiency was not affected, however, the thermal efficiency was reduced by 14% because of the reduced calorific heating value of the NCG. This is a result of the CO to CO_2 conversion.

10 Conclusion and Recommendations

The design of CRIPS 2 was aimed at resolving the problems and limitations of CRIPS 1. The heat loss seen in CRIPS 1 reduced the overall performance of the system. This was limited by the combination of both fluidised beds into one reactor, along with the addition of high-quality insulation. The modelled heat loss from the system predicted a loss of 3,2 kW, which represents 8,4% of the total heat generated.

The high-quality energy lost in the flue gas from the CB resulted in poor overall process efficiencies of CRIPS 1. The addition of internal heat recovery in CRIPS 2 has seen predicted process efficiencies increase to 74% compared to 33% for CRIPS 1. The IHR unit should be capable of preheating the air feed to 600 °C and in doing so recovering 10,7 kW of thermal energy from the exhaust. The exhaust gases left the system at 430 °C, well above the 300 °C required to prevent condensation of corrosive compounds. It was recommended that the remaining energy in the flue gas be used to dry the biomass feed or preheat the NCG feed to the PFB, reducing the heat load. The char recovery in CRIPS 2 should improve over the CRIPS 1 recovery of 58%, since the PFB of CRIPS 2 is fluidised at 0,91 m/s rather than the 0,4 m/s in CRIPS 1. This should allow the entrainment of the char particles and their recovery in the cyclone.

The cooling system was improved with the addition of a new quencher sprayer design, which allows the necessary contact between the bio-oil recycle and the hot pyrolysis vapours. A conical design was used in the unit to generate the spray of bio-oil, thereby eliminating the high pressure drop caused by the bio-oil atomisation using the vapours. The addition of a cooling tower will provide a closed loop flow of cooling water.

The new design of the PFB side distributor should allow successful fluidisation of the pyrolysis bed and generate the rotational flow required for the correct operation. It is difficult to determine whether the operation in the actual unit is correct, and it was therefore recommended to perform CFD modelling on the pyrolysis distributor and the

flow it will generate. This, together with a scale model of the system to test different distributor designs, should be done to ensure the correct operation of the new reactor.

The energy balance of the system allowed the process to be successfully modelled and the setup of the enthalpy balance approach as an analytical tool. The accuracy of the tool was confirmed by modelling of the CRIPS 1 and comparison of the results. The bio-oil heating value for CRIPS 1 was poor and it was theorised that this was due to long vapour residence times at elevated temperatures. The analysis of CRIPS 2 derived a better quality of oil, which may be possible with a higher yield of oil, suggesting less decomposition. A comparison between the high-quality oil obtained and transportation fuels is shown in Figure 26.

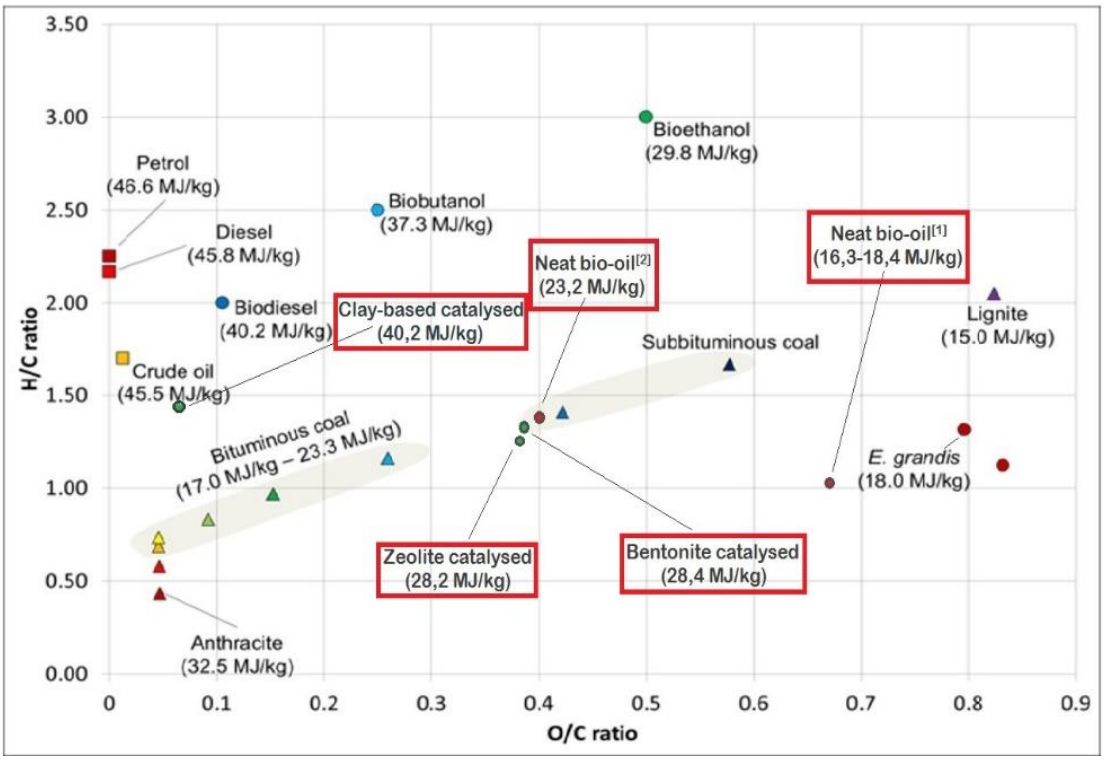

Figure 26: Van Krevelen diagram with catalysed bio-oils (Basu 2010), (Merckel 2014), (Merckel and Heydenrych 2015).

The analysis of the CRIPS 2 process with the enthalpy balance approach suggested that high thermal efficiencies can be obtained using the CRIPS design. The potential of in situ catalysis with a CRIPS process is supported by the enthalpy analysis done in Section 9, which derived good process efficiencies with the with the simulated bio-oil quality.

References

Adanez, J., A. Abad, F. Garcia-Labiano, P. Gayan, and L.F. de Diego. 2011. "Progress in Chemical-Looping Combustion and Reforming technologies." *Progress in Energy and Combustion Science* (38): 215-282.

Amutio, M., G. Lopez, J. Alvarez, M. Olazar, and J. Bilbao. 2015. "Fast pyrolysis of eucalyptus waste in a conical spouted bed reactor." *Bioresource Technology* (194): 225-232.

Basu, P. 2010. *Biomass gasification and pyrolysis: Practical design and theory.* Amsterdam: Academica Press, Elsevier.

Batcha, M.F.M., M.A.H.M. Nawi, S.A. Sulaiman, and V.R. Raghavan. 2013. "Numerical Investigation of Airflow in a Swirling Fluidised Bed." *Asian Journal of Scientific Research* (6): 157-166.

Boateng, A.A., and C.A. Mullen. 2013. "Fast pyrolysis of biomass thermally pretreated by torrefaction." *Journal of Analytical and Applied Pyrolysis* (100): 95-102.

Bridgwater, A.V. 2011. "Review of fast pyrolysis of biomass and product upgrading." *Biomass and Bioenergy* (38): 68-94.

Bridgwater, A.V., and G.V.C. Peacocke. 2000. "Fast pyrolysis processes for biomass." *Renewable and sustainable energy reviews* (4): 1-73.

Bridgwater, A.V., D. Meier, and D. Radlein. 1999. "An overview of fast pyrolysis of biomass." *Organic Geochemistry* (30): 1479-1493.

Butler, E, G Devlin, D Meier, and K McDonnell. 2011. "A review of recent laboratory research and commercial developments in fast pyrolysis and upgrading." *Renewable and Sustainable Energy Reviews* (15): 4171-4186.

Cengel, Y.A., and A.J. Ghajar. 2011. *Heat and Mass Transfer.* 4th. New York: McGraw-Hill Companies inc.

Collard, F.X., and J. Blin. 2014. "A review on pyrolysis of biomass constituents: Mechanisms and composition of the products obtained from the conversion of cellulose, hemicellulose and lignin." *Renewable and Sustainable Energy Reviews* (38): 594-608.

Demirbas, A. 2008. "Bio-fuels from Agricutural Residues." *Energy sources* (30): 101-109.

Dobele, G., I. Urbanovich, A. Volpert, V. Kampars, and E. Samulis. 2007. "Fast pyrolysis-Effect of wood drying on the yield and properties of bio-oil." *BioResources* (2): 699-706.

Fernandez-Akarregi, A.R., J. Makibar, G. Lopez, M. Amutio, and M. Olazar. 2013. "Design and operation of a conical spouted bed reactor pilot plant (25 kg/h) for biomass fast pyrolysis." *Fuel Processing Technology* (112): 48-56.

Goyal, H.B., D. Seal, and R.C. Saxena. 2008. "Bio-fuels from thermochemical conversion of renewable resources: a review." *Renewable and Sustainable Energy Reviews* (12): 504-517.

Grobler, A.B.L. 2014. *Fast Pyrolysis of Eucalyptus Grandis in a Scalable Dual Fluidised Bed Reactor System.* Pretoria: Dept. Chemical Engineering University of Pretoria.

Heidari, A., R. Stahl, H. Younesi, A. Rashidi, N. Troeger, and A.A. Ghoreyshi. 2013. "Effect of process conditions on product yield and composition of fast pyrolysis of Eucalyptus grandis in fluidized bed reactor." *Journal of Industrial and Engineering Chemistry* (20): 2594-2602.

Heinimo, J., and M. Junginger. 2009. "Production and trading of biomass for energy - An overview of the global status." *Biomass & Bioenergy* (33): 1310-1320.

Jahirul, M.I., M.G. Rasul, A.A. Chowdhury, and N. Ashwath. 2012. "Biofuels Production through Biomass Pyrolysis - A Technological Review." *Energies* (5): 4952-5001.

Kersten, S.R.A., X. Wang, W. Prins, and W.P.M. Swaaij. 2005. "Biomass Pyrolysis in a Fluidized Bed Reactor. Part 1: Literature Review and Model Simulations." *Ind. Eng. Chem. Res.* (44): 8773-8785.

Lehto, J., A. Oasmaa, Y. Solantausta, M. Kytö, and D. Chiaramonti. 2014. "Review of fuel oil quality and combustion of fast pyrolysis bio-oils from lignocellulosic biomass." *Applied Energy* (116): 178-190.

Makibar, J., A.R. Fernandez-Akarregi, M. Amutio, G. Lopez, and M. Olazar. 2015. "Performance of a conical spouted bed pilot plant for bio-oil production by poplar flash pyrolysis." *Fuel Processing Technology* (137): 283-289.

Meier, D., B. van de Beld, A.V. Bridgwater, D.C. Elliott, A. Oasmaa, and F. Preto. 2012. "State-of-the-art of fast pyrolysis in IEA bioenergy member countries." *Renewable and Sustainable Energy Reviews* (20): 619-641.

Merckel, R.D. 2014. *Fast and microwave-induced pyrolysis from Eucalyptus grandis: possibilities for upgrading.* Pretoria: University of Pretoria Dept Chemical Engineering.

Merckel, R.D., and M.D. Heydenrych. 2015. "Clay-Based in situ catalytic pyrolysis to produce high value bio-oil by decarboxylation." *TC Biomass 2015.* Chicago: TC Biomass 2015.

Nevill, J.D. 2001. *Biomass Gasification feed system: Design and Evaluation.* Texas: Graduate Faculty of Texas Tech University.

Rhodes, M. 2008. *Introduction to Particle Technology.* Second. Chichester: John Wiley and Sons Ltd.

Seider, W.D., J.D. Seader, D.R. Lewin, and S. Widagdo. 2010. *Product and Process design Principles.* 3rd. Hoboken: John Wiley & sons Pte Ltd.

Shafizadeh, F., and P.P.S Chin. 1977. "Thermal degradation of wood." In *Wood Technology: Chemical Aspects*, 57-81. I.S. Goldstein (Ed.).

Sharifzadeh, M., CJ. Richard, K. Liu, K. Hellgardt, and D. Chadwick. 2015. "An integrated process for biomass pyrolysis oil upgrading: A synergistic approach." *Biomass and Bioenergy* (76): 108-117.

Sinnott, R., and G. Towler. 2010. *Chemical Engineering Design.* 5th. Oxford: Butterworth-Heinemann.

Swart, S.D. 2012. *Design, Modelling and Construction of a Scalable Dual Fluidised Bed Reactor for the Pyrolysis of Biomass.* Pretoria: Dept Chemical engineering University of Pretoria.

van Krevelen, D.W. 1950. "Graphical-statistical method for the study of structure and reaction processes of coal." *Fuel* 269-284.

Wanicka, L.M., and M.D. Heydenrych. 2014. "Hydrodynamics of Fluidization in an Annular Space." *Industrial Fluidisation South Africa* 249-256.

Zhang, L., R. Liu, R. Yin, and Y. Mei. 2013. "Upgrading of bio-oil from biomass fast pyrolysis in China: A review." *Renewable and Sustainable Energy Reviews* (24): 66-72.

Appendix A

CRIPS 1 process flow (Grobler 2014).

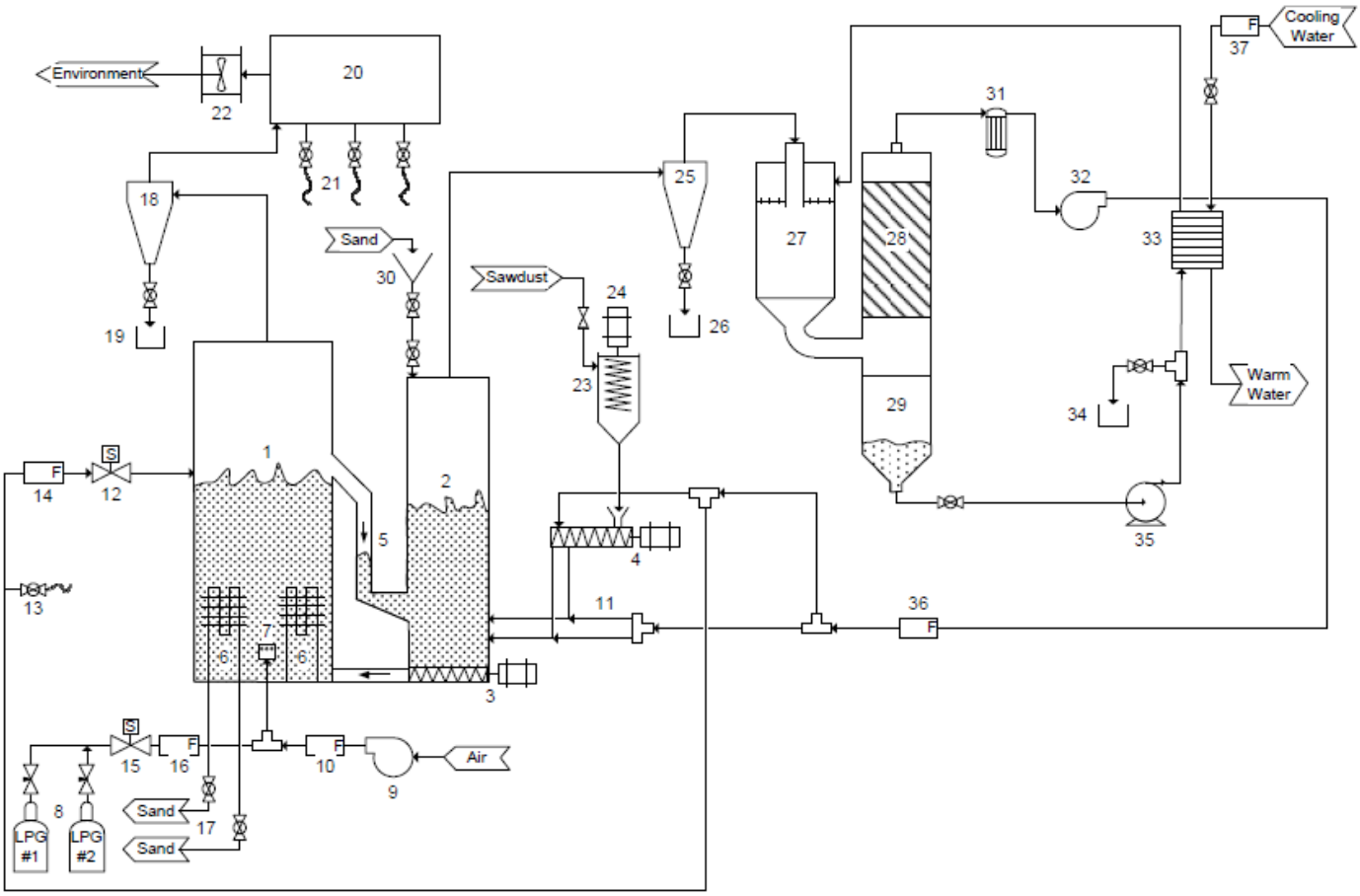

Item No.	Description	Item No.	Description
1	Combustion fluidised bed	20	Extraction/dilution box
2	Pyrolysis fluidised bed	21	Flexible air hoses
3	Sand screw feeder	22	Extraction fan
4	Biomass screw feeder	23	Biomass hopper
5	Overflow standpipe (z-valve)	24	Biomass agitator
6	Electrical heating elements	25	Bio-char cyclone
7	Bubble cap distributor	26	Bio-char container
8	LPG cylinders	27	Quencher
9	Air blower	28	Demister
10	Air flow transmitter	29	Bio-oil cyclone/container
11	Pneumatic biomass feeder	30	Sand replenish hopper
12	NCG purge solenoid valve	31	Cartridge filter
13	NCG sample point	32	NCG blower
14	NCG purge flow transmitter	33	Brass plate heat exchanger
15	LPG solenoid valve	34	Bio-oil container
16	LPG flow indicator	35	Bio-oil pump
17	Sand drains	36	NCG flow transmitter
18	Ash cyclone	37	Water flow transmitter
19	Ash container		

Appendix B

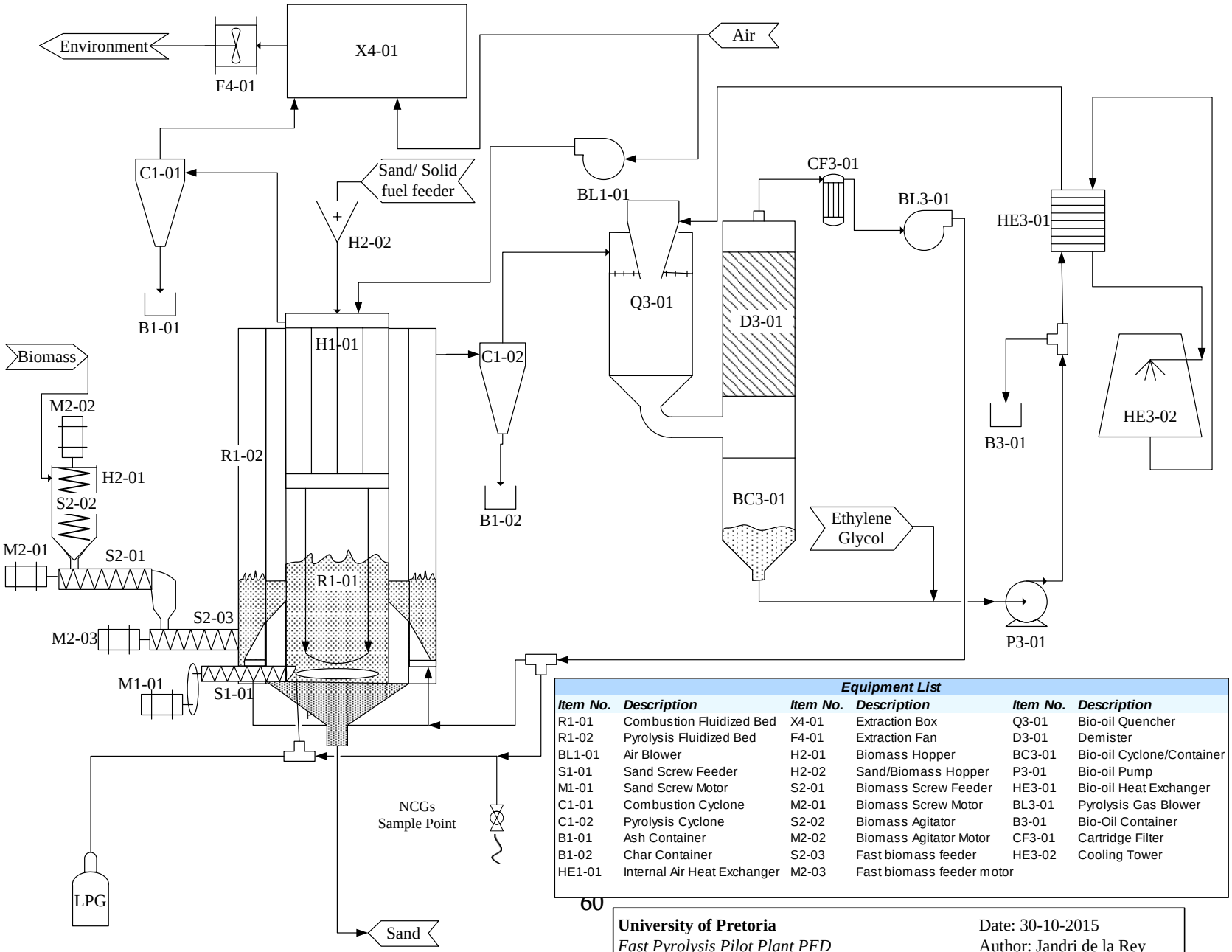

Equipment List

Item No.	Description	Item No.	Description	Item No.	Description
R1-01	Combustion Fluidized Bed	X4-01	Extraction Box	Q3-01	Bio-oil Quencher
R1-02	Pyrolysis Fluidized Bed	F4-01	Extraction Fan	D3-01	Demister
BL1-01	Air Blower	H2-01	Biomass Hopper	BC3-01	Bio-oil Cyclone/Container
S1-01	Sand Screw Feeder	H2-02	Sand/Biomass Hopper	P3-01	Bio-oil Pump
M1-01	Sand Screw Motor	S2-01	Biomass Screw Feeder	HE3-01	Bio-oil Heat Exchanger
C1-01	Combustion Cyclone	M2-01	Biomass Screw Motor	BL3-01	Pyrolysis Gas Blower
C1-02	Pyrolysis Cyclone	S2-02	Biomass Agitator	B3-01	Bio-Oil Container
B1-01	Ash Container	M2-02	Biomass Agitator Motor	CF3-01	Cartridge Filter
B1-02	Char Container	S2-03	Fast biomass feeder	HE3-02	Cooling Tower
HE1-01	Internal Air Heat Exchanger	M2-03	Fast biomass feeder motor		

University of Pretoria Date: 30-10-2015
Fast Pyrolysis Pilot Plant PFD Author: Jandri de la Rey

Appendix C